OPTIMAL ORBIT INSERTION STRATEGIES USING
COMBINED HIGH AND LOW THRUST
PROPULSION SYSTEMS

THESIS

Darren W. Johnson, Captain, USAF

AFIT/GSO/ENY/97D-02

19980128 114

DTIC QUALITY INSPECTED 3

Approved for public release; distribution unlimited

OPTIMAL ORBIT INSERTION STRATEGIES USING COMBINED HIGH AND LOW THRUST PROPULSION SYSTEMS

THESIS

Presented to the Faculty of the Graduate School of Engineering

of the Air Force Institute of Technology

Air University

In Partial Fulfillment of the Requirement for the Degree of

Master of Science in Space Operations

Darren W. Johnson, B.A.

Captain, USAF

December 1997

OPTIMAL ORBIT INSERTION STRATEGIES USING
COMBINED HIGH AND LOW THRUST
PROPULSION SYSTEMS

Darren W. Johnson
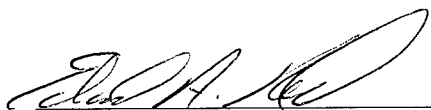Captain, USAF

Approved:

_____

Stuart C. Kramer, Lt Col, USAF

1 DEC 97

Date

_____

Edward A. Pohl, Major, USAF

1 DEC 97

Date

_____

Gregory S. Agnes, Captain, USAF

1 Dec 97

Date

Acknowledgements

I am greatly indebted to my thesis advisor, Lieutenant Colonel Stuart C. Kramer, for his insight and guidance throughout the duration of this thesis effort. His knowledge and support were greatly appreciated. I would also like to thank Terry Galati from the Propulsion Directorate, Phillips Laboratory, Edwards AFB and Steven Oleson of NYMA Inc. who spent their valuable time answering my many questions and providing additional assistance when necessary.

I would also like to thank my wife, Julie, for her love and support. It must have seemed that I was spending more time with a computer than with her over the last eighteen months, but she understood and encouraged me none the less. During this AFIT assignment, the birth of our first child, Brice, has also served in keeping our spirits high, even when graduation day seemed an eternity away.

Darren W. Johnson

Table of Contents

List of Figures

vii

List of Tables

AFIT/GSO/ENY/97D-02

Abstract

Low thrust electric propulsion systems are becoming sufficiently mature to consider their use as primary propulsion for orbital transfer in place of high thrust chemical systems. Instead of facing an either/or situation, it may be advantageous to use both types. This effort demonstrates a technique for finding orbital transfer strategies that use both high and low thrust propulsion systems and which result in optimal tradeoffs of the performance parameters cost of orbit insertion, total orbit transfer time, and available spacecraft mass at final orbit. These performance parameters are calculated as a function of the fraction of orbit transfer from Low Earth Orbit (LEO) to Geosynchronous Earth Orbit (GEO) provided by electric propulsion. Utility analysis is used to analyze each performance parameter and compute a total utility score for each orbit insertion strategy examined. Results from a variety of example space mission profiles yielded optimal orbit insertion strategies requiring both chemical and electric propulsion to provide a fraction of the LEO to GEO orbit transfer.

OPTIMAL ORBIT INSERTION STRATEGIES USING COMBINED HIGH AND LOW THRUST PROPULSION SYSTEMS

I. Introduction

Changing the trajectories of spacecraft has nearly always been a task assigned to chemical propulsion systems. Chemical propulsion systems are *endogenous*, relying on energy stored solely within the propellants to create thrust. As a result, spacecraft maneuvers requiring large amounts of energy must also require large quantities of propellant. The propellant required for most onboard chemical propulsion systems is thus a dominant mass driver. Figure 1 depicts the mass fractions of several typical spacecraft. These mass fractions clearly demonstrate the huge mass impact of onboard chemical propulsion systems.

Earth Science   **Planetary**   **GEO Comsat**
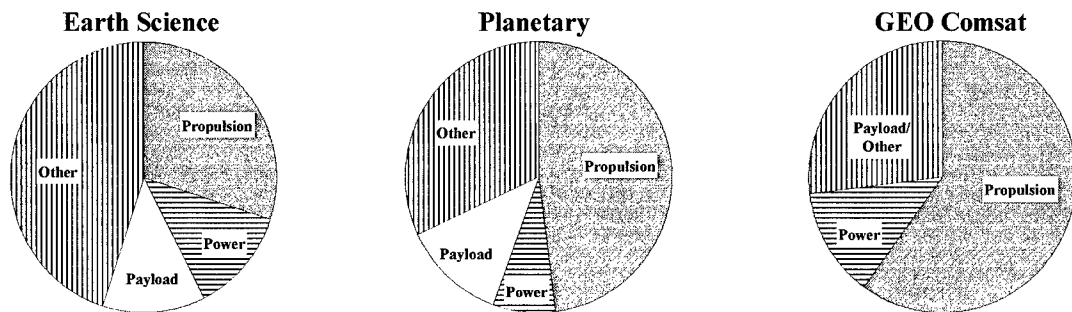
Figure 1. Typical spacecraft mass fractions (2:10)

An alternative to the endogenous chemical propulsion system is an electric propulsion system. Electric propulsion systems are *exogenous*, meaning energy is supplied to the propellant from an outside source. Since the external energy being

1

supplied to the propellant can far exceed the energy from an endogenous system, the specific impulse (I_{sp}) of an electric propulsion system is typically much greater than that of a chemical system. This higher I_{sp} gives the electric propulsion system an advantage by enabling it to maneuver spacecraft using far less propellant than the conventional chemical system. Since the dry weights of the two systems are similar, the total mass of the electric propulsion system is much less than that of the chemical system. This mass savings can be utilized typically in one (or more) of three ways: 1) to prolong the service life of the spacecraft, 2) to increase the spacecraft's payload performance, and/or 3) to shift to a less expensive launch vehicle.

A notable disadvantage of the electric propulsion system when compared to a chemical system is the time required for identical maneuvers. As with most exogenous systems, electric propulsion produces a thrust of several orders of magnitude less than that of a chemical system, providing only modest acceleration of the spacecraft. Chemical propulsion systems, on the other hand, produce high thrust and can often be treated as nearly impulsive, allowing for Hohmann type maneuvers or direct orbit insertion. Consequently, what a chemical propulsion system can do in hours, an electric propulsion system must do in weeks, months, or years, depending on the system.

Until recently, electric propulsion has been rarely considered for space missions. To reap the benefits of electric propulsion, a large amount of power must be available. Most satellites have been designed with a total power budget too small for electric propulsion to be considered for onboard propulsion requirements. The recent growth in large, high-power communications satellites, however, has presented an opportunity for the use of electric propulsion devices. For example, the Hughes HS 702 spacecraft has a

10 kW power system that is planned to grow to 15 kW (29). The HS 702 uses an electric propulsion system (xenon ion) to perform all on-orbit stationkeeping maneuvers. Only 5 kg of propellant per year is required for stationkeeping, which is roughly 5 – 15% of the propellant required by a chemical system performing the same task.

While the mass savings by using electric propulsion for on-orbit stationkeeping is substantial, an even greater mass savings is available by allowing the same electric propulsion system to provide a portion of the spacecraft's final orbit insertion. The HS 702 can perform this function to a limited degree, and it is expected that an increasing number of high-power spacecraft with high-performance electric propulsion systems will employ such a maneuver.

As the use of electric propulsion systems for final orbit insertion becomes feasible for a variety of space missions, two questions may soon be asked by spacecraft mission planners. First, "Is using electric propulsion for a portion of orbit insertion the best approach for this mission?" and if so, then, "How much of the orbit insertion should the electric propulsion system provide?" This work establishes a method for answering these questions. It employs a variety of methods for establishing trade-offs of several mission attributes, namely: 1) the time required for orbit insertion, 2) the spacecraft mass available after orbit insertion, and 3) the cost of orbit insertion. These trade-offs are conducted by incrementally varying the portion of the orbit insertion provided by the launch vehicle's upper stage, the onboard chemical propulsion system, and the onboard electric propulsion system. The results demonstrate that using a spacecraft's onboard electric propulsion system for a portion of its orbit insertion (as well as on-orbit stationkeeping) is desirable for some space missions, but not for all.

3

The next chapter summarizes the previous work performed in the field of combined high and low thrust orbit transfers. Chapter 3 discusses the computer model used for this work, the various assumptions made for spacecraft and mission parameters, and the orbital insertion strategies considered. An overview of utility analysis and its application to this effort is presented in Chapter 4. Chapters 5, 6, and 7 use the orbit transfer models and utility analysis previously discussed to find optimal orbit insertion strategies when both high thrust and low thrust propulsion devices can be utilized in combination. Chapters 5 and 6 address mission scenarios when either the launch vehicle or final mass-to-orbit parameters are constrained, while Chapter 7 considers a mission when both of these parameters are allowed to vary. Finally, Chapter 8 summarizes the results of this work and discusses some significant implications.

II. Summary of Previous Work

Work published as early as 1962 addresses the combined use of both high and low thrust propulsion systems for space missions (4, 8, 24). At that time, the study of low thrust propulsion systems was relatively new and much work was performed on finding optimum control laws which minimized the total required time for low thrust maneuvers. Since it was obvious that even minimum-time low thrust maneuvers where extremely long in duration, the development of optimal control laws for combined high and low thrust maneuvers began. All of the earlier documentation found which addressed high and low thrust propulsion focused on the development of optimization methods which could somehow merge both high and low thrust maneuvers into a unified algorithm. No work was performed which found an optimum solution to the portions each propulsion system should provide for a given spacecraft maneuver; rather, these efforts focused on optimal control laws for cases in which the portion of a maneuver (e.g. amount of Δv) provided by one of the propulsion systems was known.

Since the early 1960s to the present, published works dealing with combined high and low thrust propulsion are scarce when compared to the works for low thrust propulsion alone. An enormous amount of research has been conducted regarding low thrust propulsion systems in practically every facet imaginable. Subject areas include: new optimal control schemes for spacecraft maneuvers using low thrust, analysis of the benefits of low thrust propulsion for orbit insertion and/or station keeping, comparisons of competing low thrust propulsion technologies, and technology readiness updates of

various low thrust propulsion devices (2, 3, 5-7, 11, 15-17, 20-22, 30-33).

Of the scarce works available which examines the combined use of high and low thrust propulsion systems for orbit transfer, several publications by Steven R. Oleson, et al. falls closest in comparison to this effort (18, 19). Oleson uses the same numerical optimizer as this effort to examine the mission impact of using varying amounts of low thrusting electric propulsion to provide the final orbit insertion of a LEO to GEO transfer. This scenario is modeled using a variety of launch vehicles, electric propulsion systems, and power levels. While Oleson computes the optimal starting orbits for the use of electric propulsion provided by one or more chemical propulsion systems as the chemical Δv is incrementally varied, no attempt is made to optimize the quantity of chemical Δv (or electric propulsion Δv) for any particular mission. Nevertheless, from chemical and electric propulsion system and subsystem assumptions to a well-researched listing of references, the works of Oleson proved invaluable throughout this effort.

In another notable work, Arnon Spitzer detailed a GEO insertion strategy using both chemical and electric propulsion which was very similar in some cases to the strategy employed by the numerical optimizer used in this effort (26: 1034-1036). Spitzer's insertion strategy involved an onboard chemical propulsion system injecting the spacecraft into a highly eccentric supersynchronous orbit while removing some of the orbital inclination (if it initially exists). Afterwards the electric propulsion system removes any remaining inclination and circularizes the orbit to GEO while simultaneously maintaining a 24-hour period. The electrical propulsion system also provides thrust in a fixed inertial orientation. While the electrical propulsion system could be used to provide a varying

6

portion of the orbit insertion, Spitzer noted but did not explore this possibility or attempt to find an optimal chemical-electric propulsion system combination.

The advantages (and disadvantages) of employing an electric propulsion system to provide some portion of an orbit transfer have been addressed in previous works, as mentioned above. However, finding the optimal portion of an orbit insertion to be provided by electric propulsion has not been considered in any previous works. This may stem from the fact that there are no universal answers to such a task since the optimal portion of electric-propulsion-orbit-insertion depends largely on a number of subjective factors, such as the relative importance of cost, transfer time, and final mass to the overall mission. This effort proposes a method for finding the optimal portion of electric-propulsion-orbit-insertion by incorporating these subjective factors with a numerical optimization algorithm that models an orbit transfer using both high and low thrust propulsion systems. In doing this, a quantitative optimal solution may be found to a seemingly qualitative problem.

III. Background, Modeling, and Assumptions

This effort required the ability to find a spacecraft's optimal orbital trajectory as it is transferred from some initial orbit to a final orbit. In most cases, both high thrust chemical propulsion systems and a low thrust electric propulsion system were incorporated so that each provided a portion of the orbit transfer. This chapter presents an overview of the computer model used for this task, the assumptions made, and the orbital insertion strategies considered.

3.1 Computer Model

This effort used an existing numerical optimization computer program called Solar Electric Propulsion Steering Program for Optimal Trajectory (SEPSPOT) (23:1-69). First developed in the early 1970s under contract for the National Aeronautics and Space Administration (NASA), and subsequently revised several times with improvements since then, it is regarded as a standard for electric propulsion numerical optimization programs (31:3).

SEPSPOT calculates time optimal trajectories provided the spacecraft has no attitude constraints. It calculates a minimum propellant trajectory (which is nearly time optimal as well) if the spacecraft has attitude constraints which may limit power availability when using solar arrays. An initial high thrust stage can be included as an option with SEPSPOT. Also available as options are Earth-Sun distance effects, an analytical radiation and power degradation model, Earth oblateness perturbations, and shadowing of the spacecraft with or without thruster startup delays.

Since this effort requires varying the amounts of chemical and electric propulsion provided during an orbit transfer so that an optimal combination may be found, the high thrust option for the code was employed extensively. SEPSPOT requires that the initial orbit be circular when using the high thrust option. The amount of high thrust Δv is specified by the user and SEPSPOT allows one or two impulsive burns to find the minimum fuel trajectories. Since this transfer always requires less than one orbital revolution to complete, its time is negligible compared to the low thrust phase and is ignored. The resulting orbit after the high thrust phase is not constrained to be circular and will have semimajor axis, inclination, and eccentricity specified by SEPSPOT. The resulting orbit after the high thrust phase is optimized by SEPSPOT to provide the minimal electric propulsion transfer time.

The shadowing option was included for this effort since it was assumed that solar arrays will provide all electrical power to the thrusters during the transfer. The earth's shadow is modeled as a cylinder by SEPSPOT and its effects are calculated by turning the thrust off while in shadow. While a delay in full power operation by the thrusters as the spacecraft exits the shadow is presumably realistic and capable of being modeled with the code, it was assumed that full power operation is immediately achievable for this effort and no delay times were considered.

The effects of radiation degradation to the solar arrays when traversing the Van Allen belts is a dominant driver when selecting how much of an orbit transfer should be provided by electric propulsion. Consequently, the radiation degradation option was always enabled. SEPSPOT calculates both electron and proton radiation degradation by modeling equivalent 1 MeV electron flux as a function of orbital radius and latitude. The

total accumulated particle fluence is calculated throughout the orbital trajectory (1 MeV electron flux values are averaged over one-day intervals in the model) and the available power is constantly adjusted. SEPSPOT cannot vary the I_{sp} or the operational efficiency of the electric thrusters (they are considered constants throughout the transfer); as a result, the thrust is simply throttled as the input power is varied from the effects of array degradation. The version of SEPSPOT used for this effort allows the user to specify solar cell thickness, shielding thickness (both front and back), and base resistivity for either silicon or gallium arsenide (GaAs) solar cell types.

Regardless of the options included while using SEPSPOT, the method used to generate the trajectory was fundamentally the same. The low thrust portion of the trajectory was generated by first developing an averaged form of the Hamiltonian. Averaging the Hamiltonian yields a first approximation to the state and costate and eliminates any short period variations they may have. Averaging can be used when the state contains slowly varying orbital elements, which is the case when low thrust propulsion is used. The averaged Hamiltonian is defined as

$$\tilde{H} = \frac{1}{T} \int_{t-\frac{T}{2}}^{t+\frac{T}{2}} H\, dt \tag{1}$$

where H is the unaveraged Hamiltonian and T is the orbital period. After the averaged Hamiltonian is developed (containing the necessary constraints from the options selected), a control is calculated (the thrust direction) and the equations for the state and costate are found. When an initial high thrust phase is considered, a minimum time low thrust transfer with a specified high thrust increment is derived. The high thrust phase of the trajectory is found by solving for the optimal one or two impulsive thrusts that

10

provides the greatest change in orbital elements within a user-specified velocity increment (and using a Hamiltonian that is not averaged). The objective functions of each phase (low and high thrust) are expressed as a function of their terminal states and costates. Interface conditions between the two phases are derived by considering the parameter optimization problem of minimizing time in the low thrust phase for a fixed velocity increment in the high thrust phase. This minimization is performed at the interface between the high and low thrust phases over all of the free states and costates.

The overall trajectory was optimized using the Newton method. Initial values of the unspecified states and costates and a guess for the total transfer time were chosen by the user. An optimum high and low thrust trajectory was then generated by integrating the state and costate through both stages, but unless the initial conditions specified by the user were extremely accurate, the optimal trajectory would have the wrong terminal state. The code then revised the initial values by using a sensitivity matrix (a partial derivative matrix consisting of the changes in the final conditions with respect to the changes in initial conditions and the changes in the final conditions with respect to the changes in final time). This resulted in a new set of initial conditions and final time and the procedure was repeated until the final condition errors were within a specified tolerance.

Using a 150 MHz IBM compatible personal computer, SEPSPOT could find an optimal trajectory using both high and low thrust phases in times ranging from a few seconds to several minutes, depending on the number of options included and the time required for the transfer (longer transfer times required longer run times). SEPSPOT demanded increasing accuracy in the user specified initial conditions as more options were included and the transfer times lengthened and would typically converge to an

11

acceptable solution only after numerous attempts were made by the user at guesses for initial conditions. Computer runs for this effort with SEPSPOT included the following options: a high thrust phase, oblateness of the earth, shadowing (without startup delay), and radiation degradation. Attitude constraints and Earth-Sun distance options were excluded.

3.2 Time of Launch

If an orbit transfer is performed using a propulsion system that cannot provide thrust while in the earth's shadow, then the time of launch of the spacecraft will affect the total transfer time. The time of day a spacecraft is launched will determine its initial longitude of the ascending node (Ω_o). The value of Ω_o will determine in part the amount of time the spacecraft must spend in the earth's shadow during each orbit. The longer the spacecraft is in shadow, the longer the total transfer time. The time of year that the spacecraft is launched will also affect total transfer time. Both the time of day and time of year must be considered together to find the optimum time of launch for a specific mission.

SEPSPOT was used to create an example of launch time's effect on total transfer time in Figure 2. This graph assumes that the entire orbit transfer was performed using solar electric propulsion (SEP). The spacecraft's attitude was unconstrained so that the optimal control law for the thrust angle would not be constrained by attitude requirements and any available sun light would always be normal to the plane of the solar arrays. The starting orbit's altitude was 185 km with 28.5 degrees inclination and the final orbit was a geostationary Earth orbit (GEO). The initial spacecraft mass was 1000 kg and initial

power was 25 kW. Five ion thrusters were assumed, each operating initially at 5 kW with I_{sp} of 3500 sec and power conversion efficiency of 0.63. The effects of Earth oblateness and Earth-Sun distance were included but not solar cell degradation. The launch date was arbitrarily chosen to be 15 July 2002.
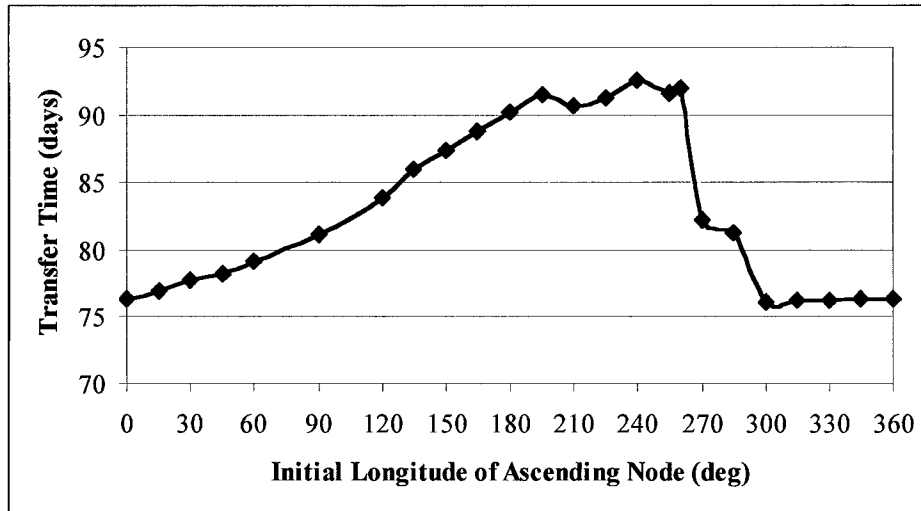
Figure 2. Transfer time as a function of initial nodal angle

From Figure 2 it is apparent that a maximum reduction of approximately 16 days in total transfer time is possible between the worst (Ω_o=240°) and best (Ω_o=300°) times to launch. Such a significant reduction in total transfer time (17.4%) would be worth taking full advantage. It should be noted that the optimum time to launch will vary depending on several spacecraft parameters (total mass, power, I_{sp}, etc.) and the above value for optimal launch time is case specific (i.e. no universal launch time exists for all spacecraft).

By repeating the graph in Figure 2 for various months in the same year, it would also become apparent that there is an optimal time of year in which to launch. Previous work in this area has shown that the optimal dates to launch are around the first day of

13

winter (21 Dec) and the first day of summer (21 Jun), but the exact date depends on the specific propulsion system used and total spacecraft mass (14:50). Both dates provide a reduction in total transfer time of up to 6% over the worst dates.

Since the precise optimal time and date of launch for spacecraft using solar-dependant propulsion systems will vary depending on a number of spacecraft parameters, it would be nice to find and use the optimal launch time for each specific spacecraft configuration used in this effort. Unfortunately, such a task is extremely labor intensive and was avoided. Instead, the same launch time was used regardless of spacecraft design parameters. Although this results in some data points being slightly more "optimal" than others (depending on how close their optimal launch time is to the launch time used), it still provided a valid basis for comparison and further study.

3.3 Electric Propulsion System

Anything which accelerates a mass by electrical heating and/or electric and magnetic field forces to provide thrust can be classified as an electric propulsion device. Nearly all electric thrusters can be grouped into three fundamental categories: 1) Electrothermal, 2) Electrostatic or Ion, and 3) Electromagnetic. Each group of electric thrusters has been used for on-orbit stationkeeping of geostationary satellites, most notably hydrazine arcjets (electrothermal) on the AT&T Telstar 4, xenon ion thrusters (electrostatic) on the Hughes HS 702 spacecraft, and stationary plasma thrusters (SPT) (electromagnetic) on the GALS Russian spacecraft (29, 34:302-306).

Since it was not the purpose of this work to analyze or compare specific electric propulsion devices, only one type was selected for modeling all orbit insertions. That

type was a xenon ion propulsion system (XIPS). The XIPS was selected due to the high I_{sp} and thrust efficiency of ion thrusters and the high performance of xenon when compared to other noble-gas propellants (21:10). It was assumed that each spacecraft configuration considered for orbit insertion would use an XIPS for all on-orbit stationkeeping. If the XIPS also provides a portion of the orbit transfer, it was assumed that the spacecraft would utilize the same XIPS for stationkeeping. Five 25-centimeter gimbaled thrusters were included, each operating at a range of $4 - 7$ kW, which is the power into the power processing unit (PPU). All power from the solar arrays was presumed to be divided equally among each thruster's PPU at all times. An I_{sp} of 3500 seconds and a thruster efficiency of 0.66 were used for all cases (16:4). A tankage fraction of 0.13 was used to account for any additional dry mass which must be added to the XIPS when it performs a portion of the orbit insertion (25:660). No additional components were added to the XIPS for redundancy or to allow for limited operating lifetimes, and it was assumed that the operational lifetimes of each component were adequate for any orbit insertion scenario.

3.4 Onboard Chemical Propulsion System

An onboard chemical propulsion system is typically used to provide the final orbit insertion to GEO after the launch vehicle's upper-stage has placed the spacecraft in a geostationary transfer orbit (GTO). For this effort, an advanced liquid bipropellant engine was assumed with an I_{sp} of 340 seconds and a dry mass of 50 kg (25:646). The tankage fraction was assigned a value of 0.1 (25:660). If the electric propulsion system provided the entire orbit transfer after the final burn from the launch vehicle's upper

15

stage, then the mass of the onboard chemical propulsion system was subtracted from the spacecraft.

3.5 Power

Although various technologies can be used to generate power for an electric propulsion system, such as nuclear, solar thermal, and solar electric, virtually all current and anticipated earth orbiting spacecraft rely upon solar electric power systems. Consequently, only a solar electric power system was considered for this effort. Of the various photovoltaic technologies available for solar electric orbital insertion, SEPSPOT could only model the degradation effects of conventional silicon or GaAs solar cells. As a result, a GaAs solar array was selected due to its superior power conversion efficiency and tolerance to radiation degradation compared to silicon. It should be noted that this is not the preferred choice of all solar cell technologies in all cases. Conventional GaAs arrays will compare favorably to other advanced technologies in terms of cost per watt and mass per watt at beginning of life (BOL) before the cells have degraded. If a significant portion of a GEO orbit insertion is performed using low thrust, however, conventional GaAs arrays could degrade more substantially than other types of solar cells and yield comparatively worst cost per watt and mass per watt values afterwards. Some other advanced photovoltaic technologies, such as concentrator or high efficiency indium phosphide solar cells, could feasibly become the preferred choice for power as more of the orbit transfer is performed by electric propulsion.

Shielding requirements of the solar cells could also vary. For the purpose of this work, all orbit transfer scenarios used 10-mil fused silica for front shielding and the back

side shielding was assumed infinite due to the array structure. This is representative of shielding values currently used on satellites with short transfer times. As the transfer times increase, however, shielding would normally be increased to allow for larger electron and proton fluence levels. By holding the shielding constant to the above mentioned values, the front side is subjected to larger fluence levels than more heavily shielded arrays, while the back side is subjected to less. This kept the model simpler to run for scenarios involving a wide range of electron and proton fluence levels while giving reasonably consistent and comparable results.

20 kW was assumed to be the beginning operational power requirement for the spacecraft after reaching GEO. To account for degrading solar arrays as the transfer time increased, the arrays were oversized at the start of the transfer so that total power output at the end of the transfer would be 20 kW. The specific mass of the GaAs solar arrays was set at 60 W/kg (21:12). A mass penalty was assessed to the electric propulsion portion of the orbit transfer due to the oversized solar arrays at 16.67 kg/kW.

3.6 Orbit Insertion Strategies

In order to avoid the cost of larger launch systems which could inject a GEO satellite directly into final orbit, many GEO satellites use a smaller launch vehicle to place them in a geostationary transfer orbit (GTO) instead. Once in GTO, the launch vehicle's upper stage is separated from the spacecraft and an onboard chemical propulsion system is used to circularize the final orbit and remove inclination with one or more burns at apogee. An alternative is to employ an onboard electric propulsion device for final orbit insertion either directly after the spacecraft is placed into GTO, or

sometime after the onboard chemical propulsion system has provided a portion of the final transfer.

For this effort, orbit transfers were modeled by allowing the portion of the final orbit insertion provided by solar electric propulsion (SEP) to vary by discrete increments. The conventional case in which an onboard chemical propulsion system provides the entire final transfer from GTO to GEO is first calculated. Next, propellant (in the form of Δv) is incrementally off-loaded from the onboard chemical propulsion system and added to the SEP system. This continues until the onboard chemical system has no propellant left and the transfer from GTO to GEO is conducted entirely by electric propulsion. At this point, the process continues with propellant being off-loaded from the launch vehicle's upper stage in exchange for SEP propellant. This allows the SEP system to take over at orbits requiring less energy than GTO. This incremental process continues until the SEP system is providing the entire orbit transfer from just a low Earth parking orbit. While extreme mass savings are gained at this point, it is done at the cost of long transfer times and severe punishment through the Van Allen belts. Nevertheless, an entire orbit transfer using SEP is a valid scenario and is included as the last case.

While it was easy to find sources which list the maximum weight that can be launched to low earth orbit (LEO) and GTO by a variety of launch vehicles and upper stages, at various increments the maximum weight launched to orbits in between LEO and GTO were needed as well. Since these values proved difficult to obtain, the rocket equation was used to approximate them and appears below.

$$m_f = m_o e^{\frac{-\Delta v}{gI_{sp}}} \tag{2}$$

18

Eq (2) is an ideal case and does not account for gravity and drag losses. To account for this, known values for the maximum weights launched to LEO and GTO were used to scale Eq (2). The scaling factor was found by simply adjusting the Δv supplied by the launch vehicle's upper stage so that Eq (2) closely approximated the known maximum weights launched to LEO and GTO. Once the scaling factor was found for a particular launch vehicle, the maximum launched weights to points in between LEO and GTO were calculated with modest accuracy. These mass values were used as the starting spacecraft mass for the SEP system. For cases where the SEP system started beyond GTO, Eq (2) was used with the assumed performance parameters of the onboard chemical propulsion system (sec. 3.4).

Regardless of the launch vehicle under consideration, it was assumed that the upper stage would first be used to insert into a 300 km circular orbit with 28.5° inclination. 300 km was arbitrarily chosen as a representative LEO parking orbit altitude, while 28.5° represents the inclination of vehicles launched from Cape Canaveral, FL. After reaching parking orbit, the upper stage would incrementally raise the orbit's apogee until GTO was obtained. The inclination was slightly decreased with each increment. The result was a GTO with perigee altitude at 300 km, apogee altitude at 35,786 km, and inclination at 26.5°. An illustration of the primary orbits included for this effort and representative SEP starting orbits are displayed in Figures 3 and 4 below.

GTO

GEO

300 km LEO

Example SEP
Starting Orbit
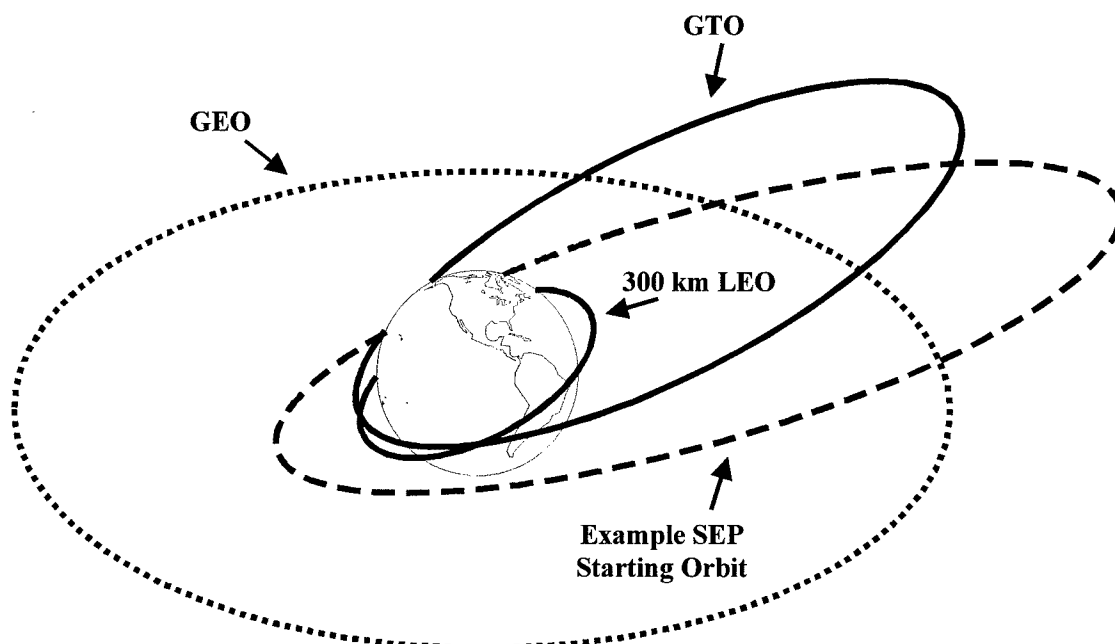
Figure 3. Primary orbits included in the LEO to GEO orbit insertion process

GEO

GTO
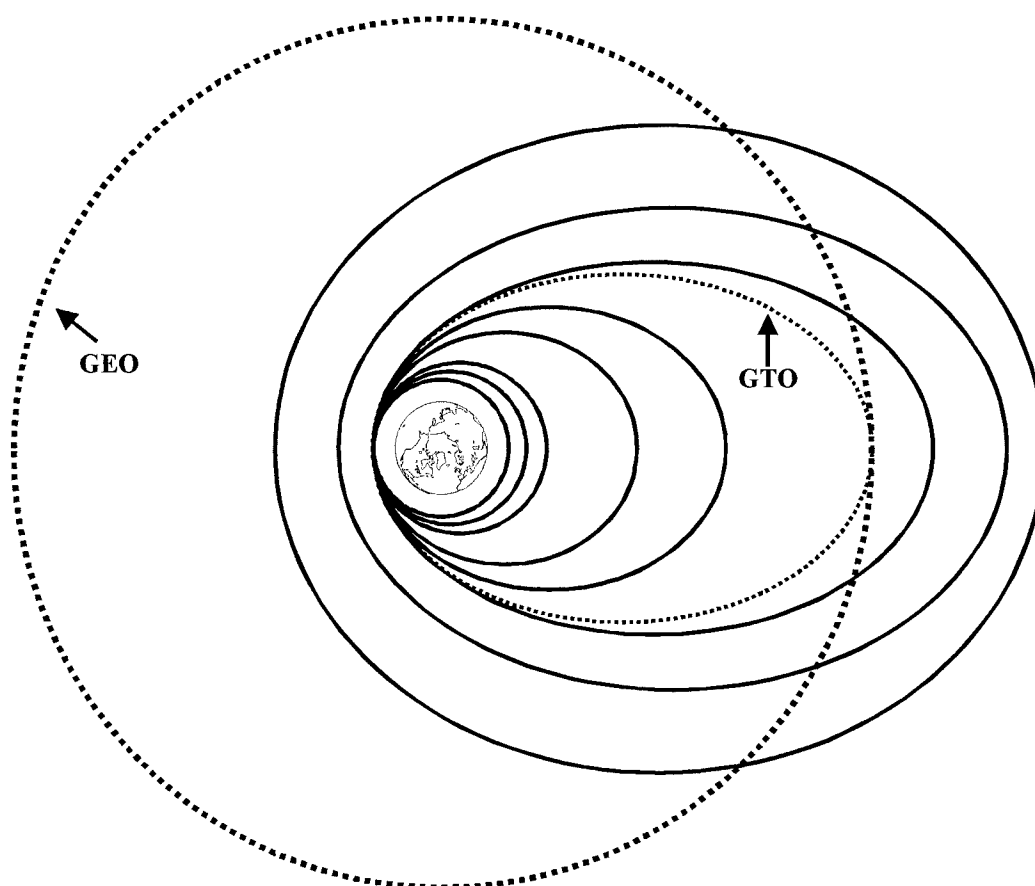
Figure 4. A sampling of SEP starting orbits as seen from above the North Pole

20

Figure 3 depicts a scenario in which the SEP system is employed after an onboard chemical system has provided a partial transfer from GTO. Figure 4 displays a variety of SEP starting orbits as the portion of the transfer from either the launch vehicle's upper stage or the onboard chemical propulsion system is incrementally varied. It is interesting to note that once in GTO, SEPSPOT uses the Δv provided by the onboard chemical propulsion system to raise the orbit's apogee above GEO altitude while also raising perigee (inclination begins to substantially be reduced at this point as well). This serves to decrease the spacecraft's velocity at apogee thus making it better for plane changing, while also increasing the time spent out of the damaging radiation belts.

In conjunction with finding the optimal utilization of high thrust impulsive Δv, SEPSPOT calculates the optimal steering profile used by the SEP system to minimize the total orbit transfer time. Examples of such steering profiles are included as Figures 5 and 6. Figure 5 is based on an SEP starting orbit after the onboard chemical propulsion system has provided a portion of the orbit transfer from GTO. It displays the optimal steering at various points along the first orbital path, which has an inclination of approximately 7.5°.
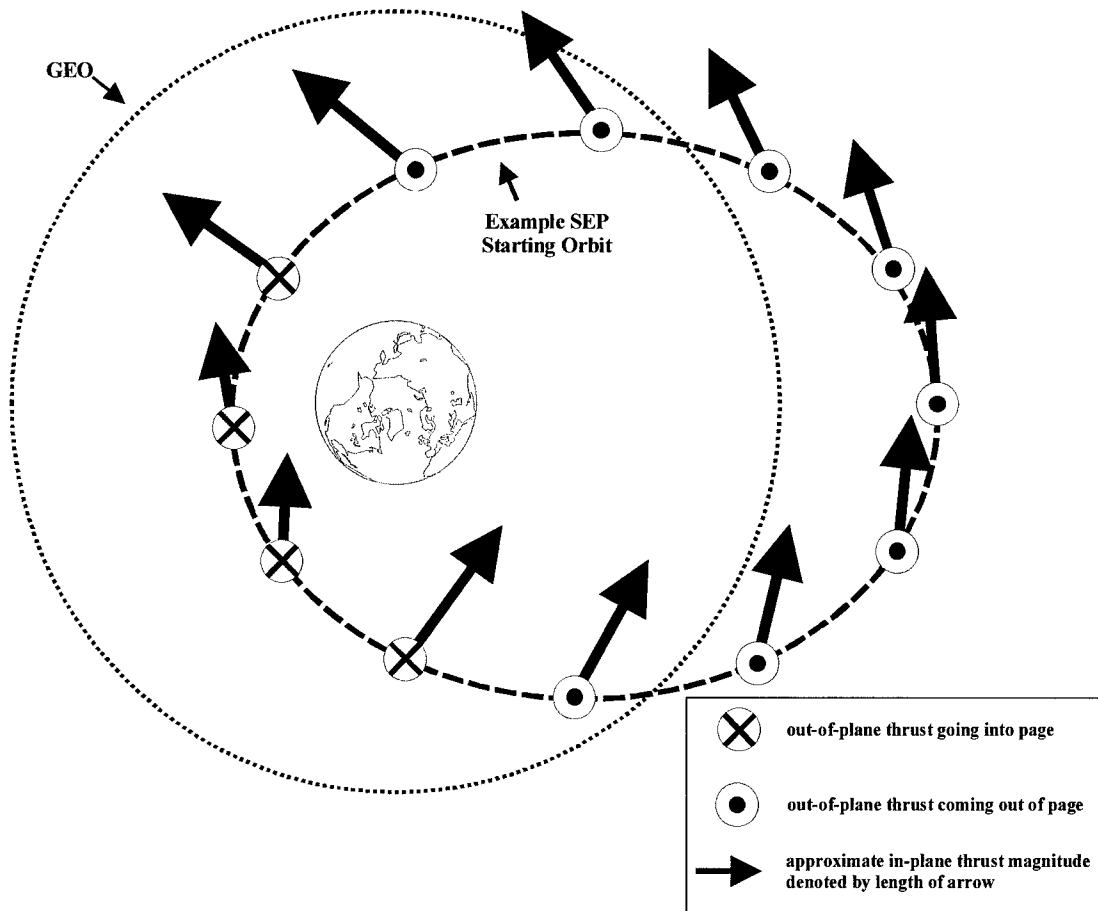
Figure 5. Optimal steering profile by SEPSPOT beyond GTO

This figure is limited by a top-down view so that only the relative magnitude of the in-plane component of thrust is displayed. The total thrust magnitude is nearly constant throughout the orbital trajectory so the out-of-plane thrust magnitude varies inversely to that of the in-plane thrust. In this particular case, the out-of-plane thrust ranges roughly between $10°$ and $50°$ in either direction from the orbit plane. It is also interesting to note that the in-plane thrust direction is roughly inertial in attitude and similar to Spitzer's orbital insertion strategy described in section 2.1.
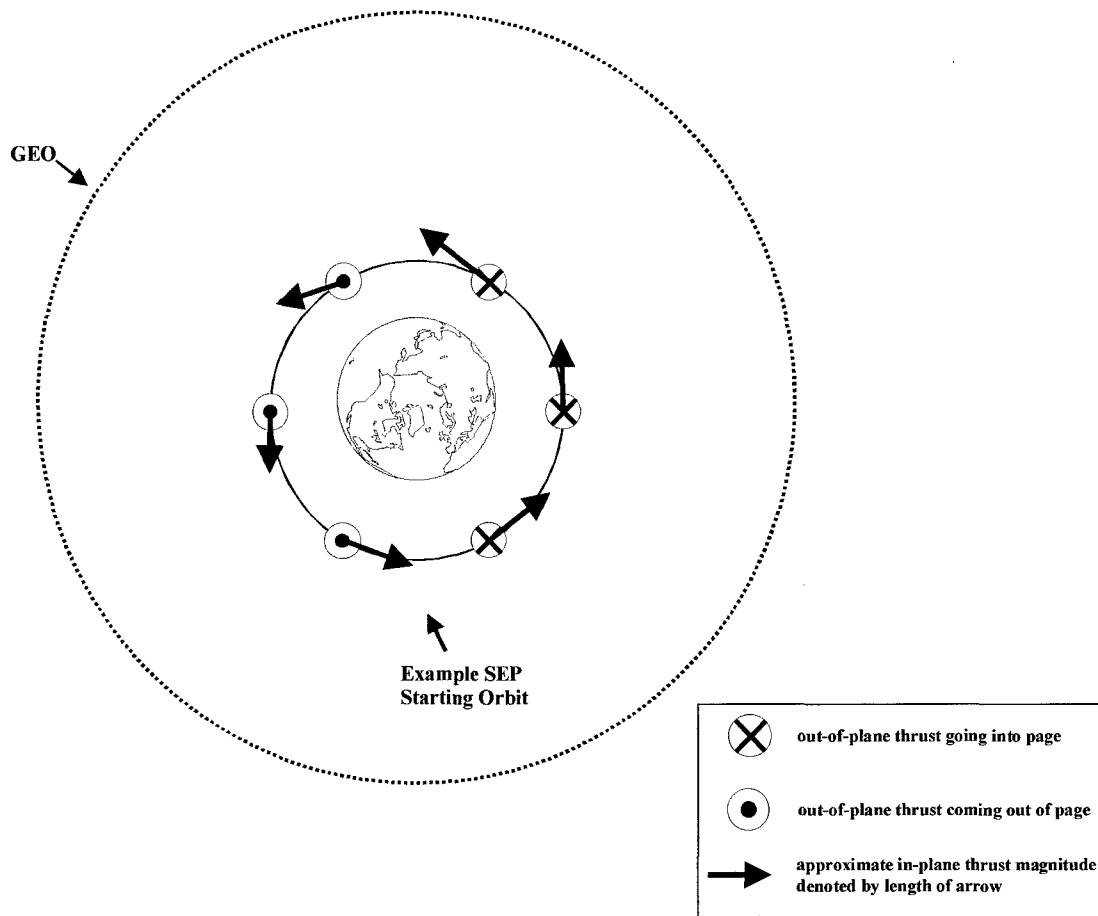
Figure 6. Optimal steering profile by SEPSPOT at LEO

Figure 6 is based on a circular 300 km SEP starting orbit in which the SEP system

provides the entire orbit transfer. It displays the optimal steering at various points along

the first orbital path, which has an inclination of 28.5°. This figure is also limited by a

top-down view so that only the relative magnitude of the in-plane component of thrust is

displayed. The out-of-plane thrust ranges roughly between 30° and 80° in either direction

from the orbit plane. In this example the optimal steering is nearly tangential to the

orbit's circular path, as most optimal control algorithms would predict for circle-to-circle

low thrust orbit transfers.

IV. Establishing Total System Utility

This effort examines three attributes that are important factors in deciding an orbit insertion strategy. These three attributes are: 1) final mass of a spacecraft delivered to its final orbit, 2) the total transfer time required, and 3) the total cost of delivering the spacecraft to its final orbit. Each of these attributes will take on different performance values as we examine a variety of orbit insertion strategies by changing the portion of the orbit transfer provided by SEP. The optimal orbit insertion strategy for a particular mission will possess the best combination of attribute performance values. As a result, the main question to answer when attempting to find the optimal orbit insertion strategy is, *How do different orbit insertion strategies, each with different combinations of attribute performance values, compare to one another?* Utility analysis can be employed to answer this question.

Utility is generally a measure of user satisfaction. For this effort, utility is a measure of how well one or more mission objectives are being satisfied. Utility scores are derived from utility functions. Utility functions take raw performance values (attribute values in this case) and create utility scores on a common scale for comparison. Each orbit insertion strategy not only has a unique combination of attribute performance values, but also a combination of attribute utility scores. A total system utility score for each orbit insertion strategy can be derived from the combination of attribute utility scores. It is the total system utility score that will ultimately determine which orbit insertion strategy best addresses the mission objectives collectively and is thus optimal.

For a given mission, creating a utility function for each mission attribute which best suites the mission objectives may often be a difficult task. Although the process of finding the right utility functions for a mission is not addressed in this work, there are many publications available which can aid a mission planner in this particular area (1:542-546; 12:188-212; 36:423-427). For the purposes of this work, a variety of utility functions are explored as examples.

The simplest utility function is one that follows a linear scale. This utility function is a simple equation and appears as:

$$U(x) = \frac{x - \min_x}{\max_x - \min_x} \tag{3}$$

where $U(x)$ is the utility function, x is the value of interest (such as mass, time, or cost), and max_x and min_x are the maximum and minimum values for the total range of x. A graph of this function is shown in Figure 7 below using an example attribute x which ranges in performance value from 0 (worst value) to 50 (best value). The utility values are constrained by Eq (3) to fall between zero and one so that regardless of the attribute being considered, the range of utility values will be consistent.
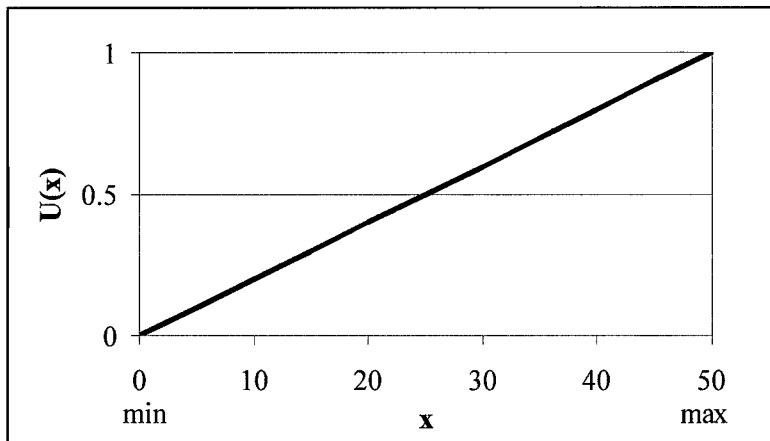
Figure 7. Utility curve from equation (3)

25

When using linear utility functions, it is assumed that any increase in the value of an attribute is just as good as an equivalent decrease is bad (or vice-versa). This would seldom be the case when planning a space mission. Typically only a limited range of values of an attribute may be favorable, and those outside the range will rapidly become less and less appealing. For this reason exponential functions are often used to model these types of utility preferences. Equations 4 – 7 and Figures 8 – 11 display typical exponential utility functions and their associated curves. These functions were used in various combinations in performing this analysis and are well suited for a wide range of applications.

$$U(x) = \frac{e^{\left(\frac{max-x}{R}\right)} - 1}{e^{\left(\frac{max-min}{R}\right)} - 1} \tag{4}$$
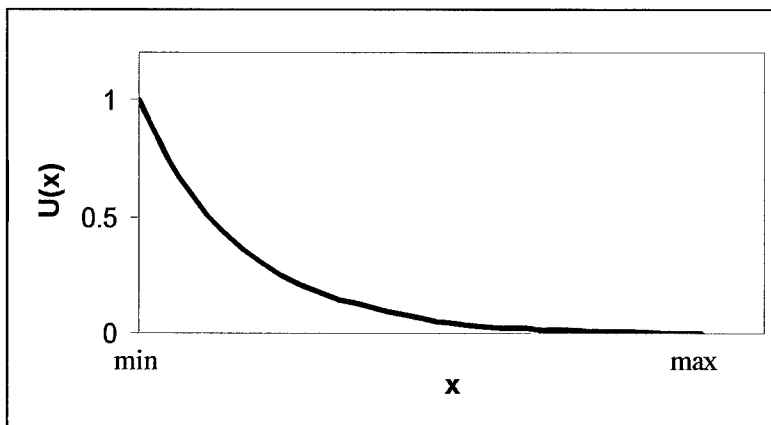
Figure 8. Utility curve from equation (4)

26

$$U(x) = \frac{e^{\left(\frac{x - \text{max}}{R}\right)} - 1}{e^{\left(\frac{\text{min} - \text{max}}{R}\right)} - 1} \tag{5}$$
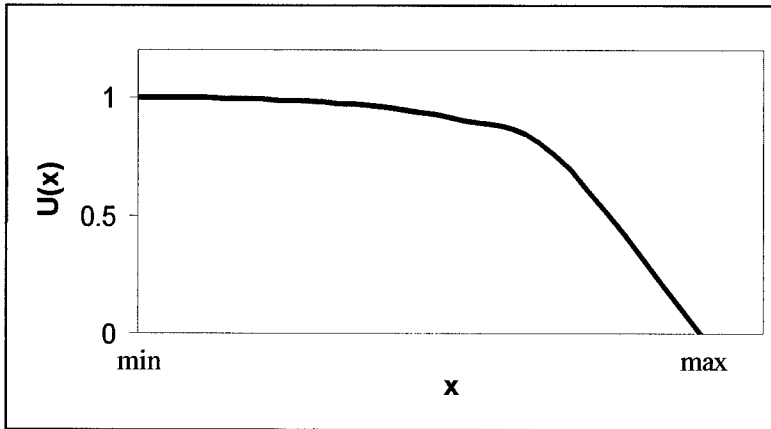
Figure 9. Utility curve from equation (5)

$$U(x) = \frac{1 - e^{\left(\frac{x - \text{min}}{R}\right)}}{1 - e^{\left(\frac{\text{max} - \text{min}}{R}\right)}} \tag{6}$$
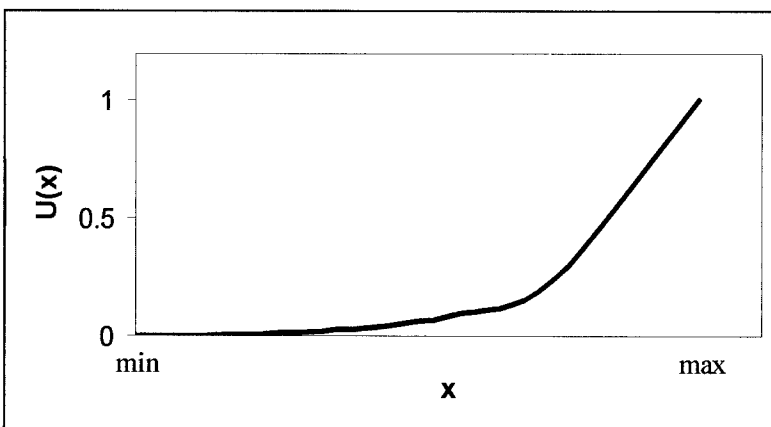
Figure 10. Utility curve from equation (6)

27

$$U(x) = \frac{1 - e^{\left(\frac{min - x}{R}\right)}}{1 - e^{\left(\frac{min - max}{R}\right)}}$$ (7)
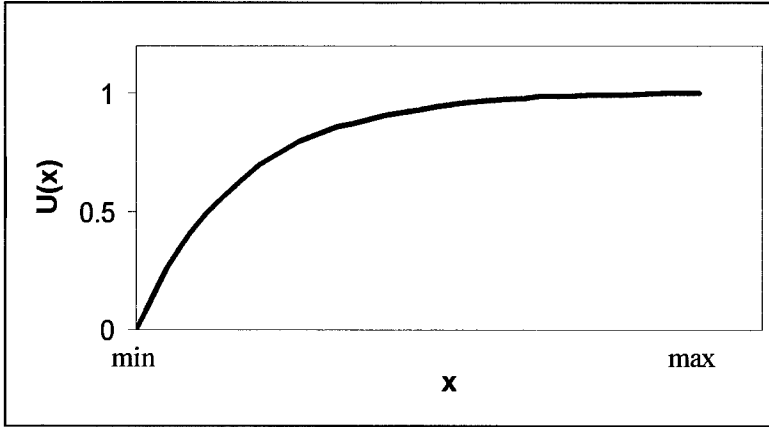
Figure 11. Utility curve from equation (7)

For equations 4 – 7, *max* and *min* are the maximum and minimum values for the total

range of x. *R* is a constant term (specified by the user) which dictates the shape of each

exponential function and allows the user to construct a curve which not only satisfies the

endpoint (max and min) conditions, but also allows an intermediate value of x to be

assigned a specified utility value.

Once a utility function is established for each attribute being considered, a total

system utility score must be computed for each orbit insertion scenario (remember that

each orbit insertion scenario requires a different amount of SEP Δv, as discussed in

section 3.6). The total utility score is obtained by combining the individual utility scores

from each of the attributes being considered. A very simple but still widely applicable

approach is to simply add the scores together.

28

The attributes for any particular mission will rarely be of equal importance. For example, the final mass delivered to orbit may be two or three times more important than the total transfer time for a specific mission. To accomplish this, the utility value for each of the mission attributes may be weighted before they are summed together for the total utility score. The following equation can be used to compute the total utility score for a specific orbit insertion scenario:

$$U_{total}(\Delta v_{SEP}) = a \cdot U_x(\Delta v_{SEP}) + b \cdot U_y(\Delta v_{SEP}) + c \cdot U_z(\Delta v_{SEP}) + ... \qquad (8)$$

where $U_{total}(\Delta v_{SEP})$ is the total utility of the orbit insertion (as a function of SEP Δv), U_x, U_y, and U_z are the utility values for various mission attributes, and a, b, and c are weightings which determine the relative importance between attributes. For this effort, the weightings where always scaled so that they sum to one, which ensures that the total utility values will consistently range between zero and one. As with the utility functions, methods for finding a suitable combination of weightings for a particular mission are not discussed in this work. Many strategies for establishing these weightings use either ranking, rating, or paired comparison schemes which are quite simple to conduct, and publications which deal with decision making strategies should be referenced for that purpose (1:546-552; 28:19-26; 36:427-430).

It should be noted that attribute independence is assumed for this effort, which enables the use of an additive total utility function in Eq (8) (1:582-585). Attribute independence basically implies that regardless of the value of some given attribute, the utility values for the other attributes will not change. If this is not the case, and the relative importance of each attribute to the mission can not be considered independently

from the others, then a different strategy must be used and Eq (8) is no longer valid.

Publications dealing with decision making strategies should be referenced in this case as

well to obtain a different system scoring approach (1:586, 592-593).

V. Optimal Orbit Transfer with Constrained Launch Vehicle

This chapter describes a method for finding the optimal combination of high and low-thrust propulsion systems for orbit transfer when the mission is constrained to use a specific launch vehicle. Two attributes, mass to final orbit and total transfer time, will be traded off in the optimization process. While the total cost of orbit insertion may vary significantly even with the launch vehicle fixed, it is not addressed in this chapter. Chapter 6 and Chapter 7 will include the cost attribute for cases where the launch vehicle is unconstrained. For the purposes of this chapter, a Delta II launch vehicle was used for all calculations.

5.1 Final Mass and Transfer Time Calculations

When the launch vehicle is constrained to a specific type, the mission planner is constrained to a maximum mass that can be launched to a specified orbit by the launch vehicle. This maximum mass varies depending on the orbit (and its associated energy) to which the payload was launched. In this chapter, the Delta II (6925) launch vehicle was selected to serve as an example. This vehicle is capable of launching a payload to a 300 km circular orbit with final mass at roughly 3850 kg, and to GTO with a final mass of 1380 kg (13:674-676). The PAM-D upper stage was assumed with a 206 seconds Isp (13:677), and all payload masses launched to intermediate orbits between LEO and GTO were approximated using the rocket equation (Eq (2)). For further details on spacecraft parameters assumed for all orbit transfers, see sections 3.4 – 3.6.

The final mass of the spacecraft once it reached its final orbit and the transfer time required were calculated as a function of the portion of orbit transfer provided by SEP in the form of SEP Δv and appear in Figures 12 and 13. The final mass of the spacecraft is calculated as a *final available mass*. Final available mass is defined as the total spacecraft mass at final orbit minus the mass from all systems solely related to the orbit transfer. It was calculated using the following equation:

$$m_a = m_t - m_{chem-engine} - a \cdot m_{chem-propellant} - b \cdot m_{SEP-propellant} - c \cdot P_{lost} \tag{9}$$

where m_a is the final available mass, m_t is the total spacecraft mass at final orbit, $m_{chem-engine}$ is the mass of the on-board chemical propulsion engine, $m_{chem-propellant}$ is the mass of the liquid propellant required by the on-board chemical propulsion system for orbit transfer, $m_{SEP-propellant}$ is the mass of the xenon propellant required by the SEP system for orbit transfer, P_{lost} is the amount of power lost due to radiation degradation during orbit transfer, and a, b, and c are chemical tankage fraction, SEP tankage fraction, and solar array specific mass respectively. Only the excess tankage and supporting structure required for the SEP portion of the orbit transfer is included in Eq (9) since it was assumed that the same SEP system would be required for orbit maintenance once the spacecraft was in operation. This method of calculating final mass serves to penalize the propulsion system combination required for orbit transfer as it becomes more massive as well as the associated damage to the solar arrays for longer trip times. This is due to the fact that once the spacecraft reaches its operational orbit, the portion of the propulsion system(s) required for orbit transfer and the damaged solar arrays can no longer be used

and represent dead weight. Final available mass is thus the quantity of *useable* mass that

the mission planner would have available to budget for the entire spacecraft once it

reached its operational orbit.
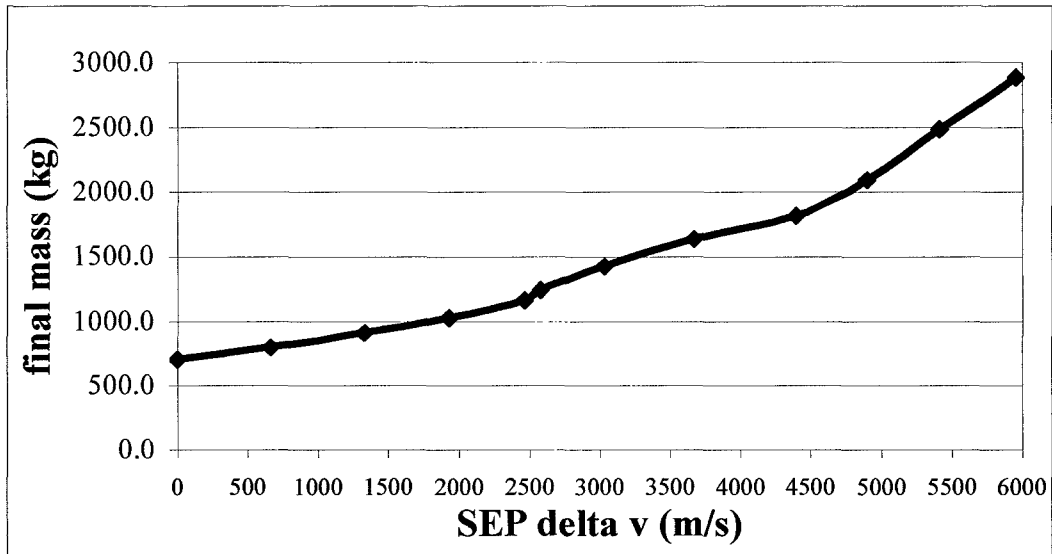
Figure 12. Final available mass as a function of SEP Δv for Delta II (6925) launch vehicle
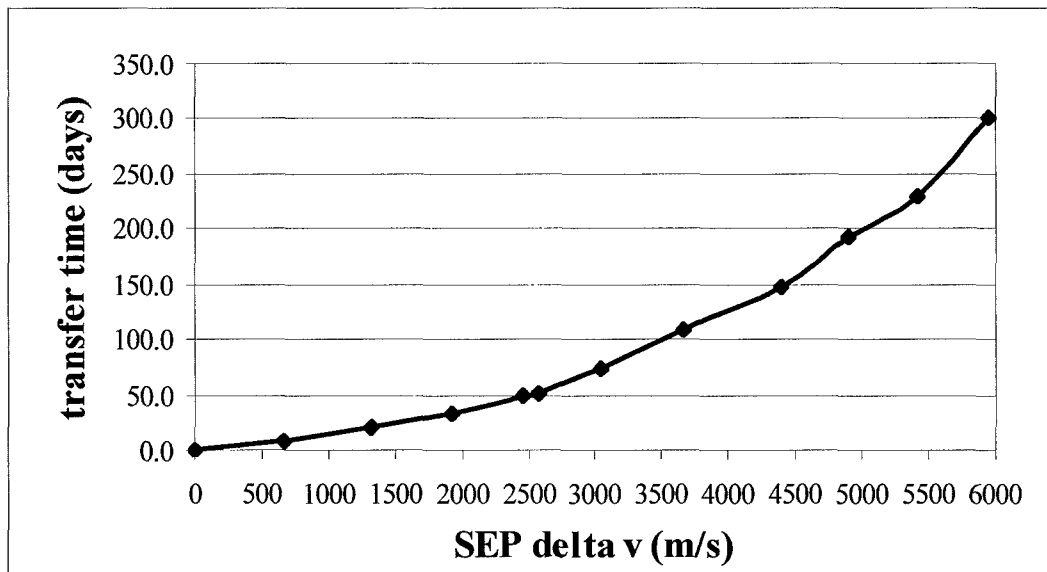
Figure 13. Total transfer time as a function of SEP Δv for Delta II (6925) launch vehicle

Figure 12 shows the final available mass as a function of the portion of the orbit

transfer provided by SEP (in the form of SEP Δv). The small jump in the curve around

the SEP Δv of 2576 m/s is at GTO. This represents the point at which the mass from the

on-board chemical propulsion system is deleted from the spacecraft (as the curve is

viewed from left to right). Figure 13 shows the total transfer time. The low sloping curve

at the smaller values of SEP Δv in Figure 13 shows that the time required for orbit transfer

grows slowly as a small portion of the final insertion is performed by SEP. Conversely,

Figure 12 shows that the steepest region of its curve (and best mass savings) occurs when

a majority of the orbit insertion is performed by SEP.

The effects of power degradation as a function of the SEP Δv used for orbit

insertion have been included as well in this section and are displayed in Figure 14. Power

degradation has an adverse effect on both total transfer time and final available mass.
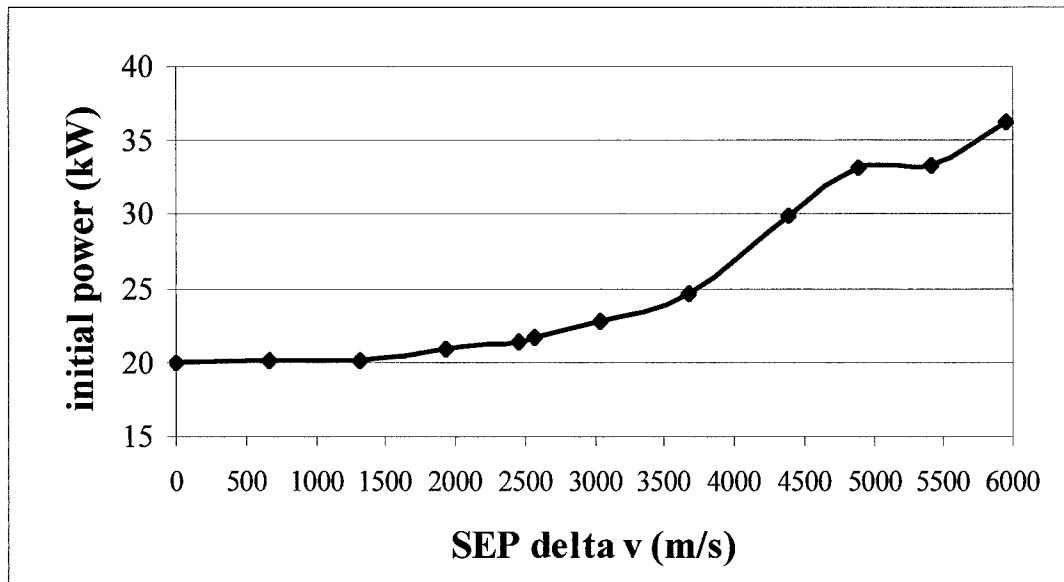
Figure 14. Initial power requirements as a function of SEP Δv

34

Figure 14 displays the amount of initial power required by the spacecraft before orbit insertion so that 20 kW will remain after the insertion is complete. The effects from the shape of this curve can be seen when examining Figure 12 and 13. The lack of substantial power degradation for SEP Δv values less than 2500 m/s contribute to the slopes of the curves in Figures 12 and 13 being slightly flatter than for SEP Δv values greater than 2500 m/s.

From observing Figures 12 and 13 together, it is easily noticed that both final mass and transfer time are directly related to the amount of SEP Δv provided. Unfortunately, it is typically favorable to maximize the final available mass while minimizing total transfer time. In this case, maximizing one simply maximizes the other, and since both are important when deciding the role of SEP for orbit insertion, a problem still remains.

Table 1 summarizes the data from which Figures 12 – 14 were constructed. Referring to this table will aid the reader in determining the characteristics of the launch strategy used at each point in many of the figures in this chapter. The column containing the values for SEP Δv for each of the orbit insertion scenarios has been highlighted. This column should be used to match a data point from the figures with its correct value of SEP Δv. The row that contains this SEP Δv value also contains other mission characteristics for that particular orbit insertion strategy.

Table 1. Performance calculations for orbit insertion with Delta II (6925) launch vehicle

orbit insertion strategy	mass after chemical orbit insertion (kg)	Electric Propulsion System				Mission Attributes	
		delta v (m/s)	propellant mass (kg)	final mass at GEO (kg)	initial power (kW)	final available mass (kg)	total transfer time (days)
Launch system to GTO, on-board chem. to GEO	807.9	0	0.0	807.9	20.0	757.9	0.0
Launch system to GTO, on-board chemical for some portion, then SEP to GEO	917.2	663	17.6	899.6	20.1	846.5	9.1
	1041.3	1324	39.4	1001.9	20.1	944.8	20.3
	1182.1	1929	64.6	1117.5	20.9	1043.5	33.5
	1342.0	2461	92.9	1249.1	21.4	1163.8	48.1
Launch system to GTO, SEP to GEO	1380.0	2576	99.8	1280.2	21.6	1240.3	52.1
Launch system from LEO (parking orbit) to intermediate orbit between LEO and GTO, then SEP to GEO	1624.7	3035	137.5	1487.7	22.8	1423.0	73.9
	1930.7	3669	195.7	1735.3	24.7	1632.7	107.5
	2294.3	4398	275.9	2019.0	29.9	1819.5	147.7
	2726.4	4892	362.2	2363.9	33.2	2097.7	192.9
	3239.8	5415	472.9	2767.1	33.4	2483.9	229.4
SEP from LEO to GEO	3850.0	5958	613.5	3236.5	36.3	2886.2	301.6

5.2 Mass and Transfer Time Utility Analysis and Optimal Solutions

The concepts of attribute utility and total utility discussed in Chapter 4 will now be applied. In this chapter there are only two attributes considered for finding an optimal orbit insertion strategy, final available mass and total transfer time. Figures 12 and 13 in the previous section displayed the values of these two attributes as a function of the portion of the total orbit insertion provided by SEP. Utility values for this data can now be determined by choosing an appropriate utility function. As previously noted, the utility function for each attribute must be determined by mission planners to reflect the mission utility of each attribute throughout the range of its possible values.

First, we will use the simple linear utility function as an example. This function was shown in Eq (3). Figures 15 and 16 show the results of using Eq (3) with the mass and time data from Figures 12 and 13.

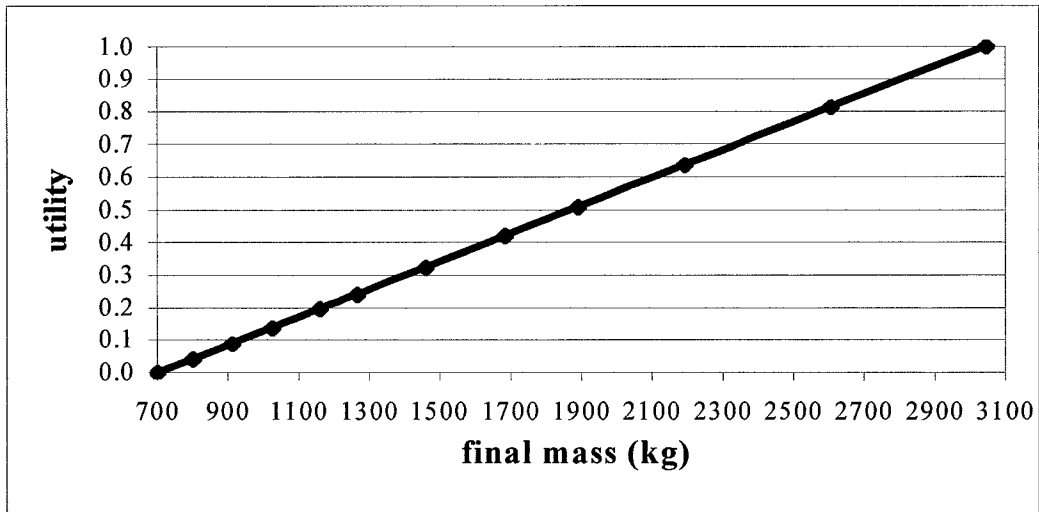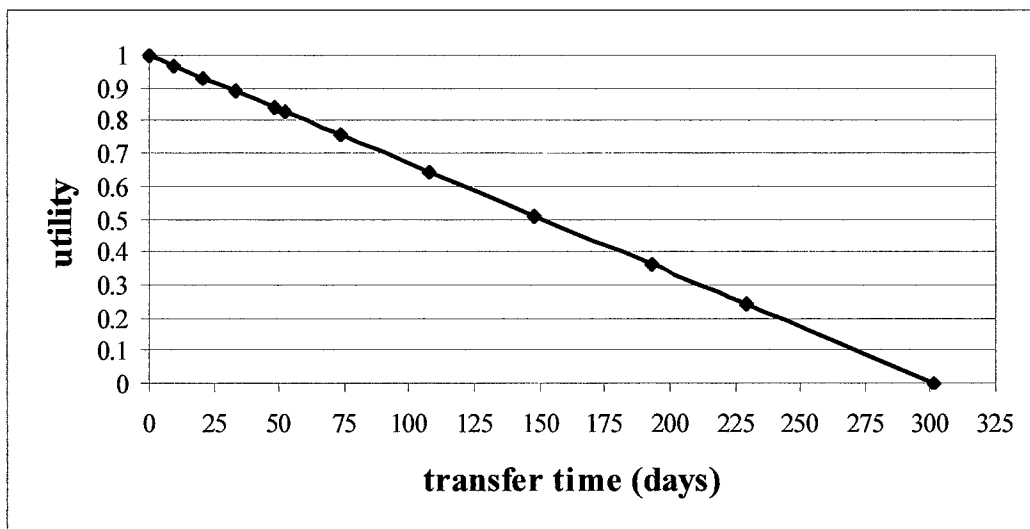**Figure 15. Final available mass utility curve (linear)**

Figure 16. Total transfer time utility curve (linear)

Figures 15 and 16 allow us to find the separate utility scores for final available mass and total transfer time throughout the entire range of each of their values. Independently, however, these utility scores are of little use and must be combined in some fashion to derive the total mission utility.

Eq (8) can now be used to establish total utility scores for the orbit insertion process as the portion of orbit insertion provided by SEP is varied. Figure 17 is a graph of the total utility score using the linear utility function for both the time and mass attributes. It contains curves generated with a variety of weighting combinations for the two attributes, representing changing relative importance of each attribute to the mission.
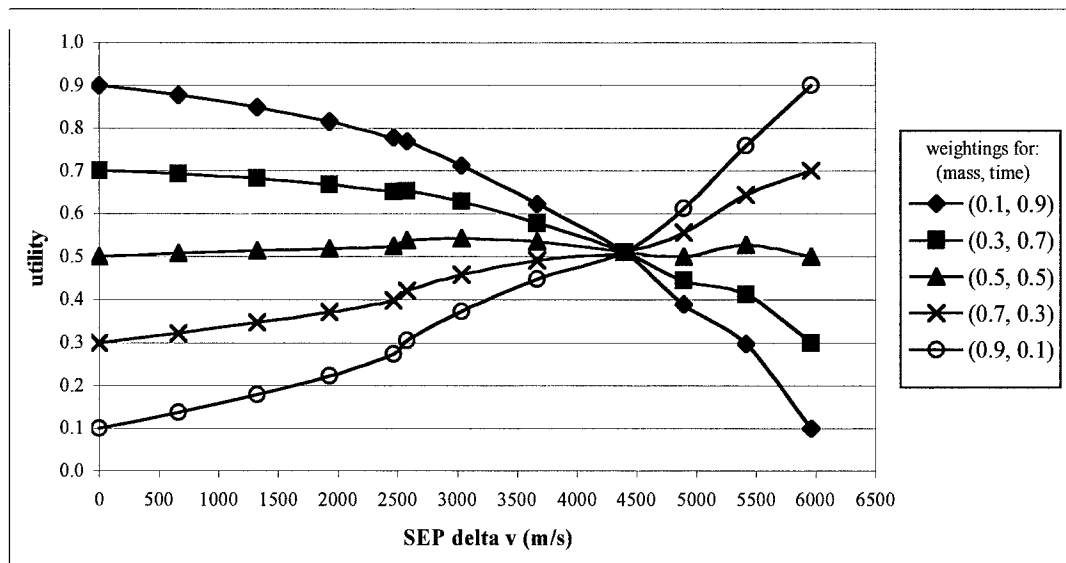
Figure 17. Total utility for orbit transfer (with linear attribute utility function)

The point of maximum total utility is the optimum orbit insertion strategy for each weighting scheme. For this example where both mass and time utilities are treated linearly, the results are fairly predictable. In the cases where final available mass is more important than transfer time, the optimum solution is to use SEP for the entire orbit transfer (LEO to GEO). In the cases where transfer time is more important, it is best to avoid SEP entirely and simply use the chemical propulsion systems. The most interesting results arise when both mass and time attributes are weighted nearly equal. In these cases,

the optimal configuration is to allow the SEP system to provide varying amounts of Δv.

These situations are shown in Figure 18. Figure 18 shows the optimal amounts of SEP Δv

provided for orbit insertion for each mass weighting in Figure 17 along with other mass

weightings that were not shown in Figure 17. The boldly highlighted data points in the

figure represent the five mass weighting values that were shown in Figure 17 while the

other data points are additional mass weightings that were included to increase the

"resolution" of the graph. Graphing the optimal points in this fashion helps to display how

the optimal orbit insertion strategies and attribute weightings relate.
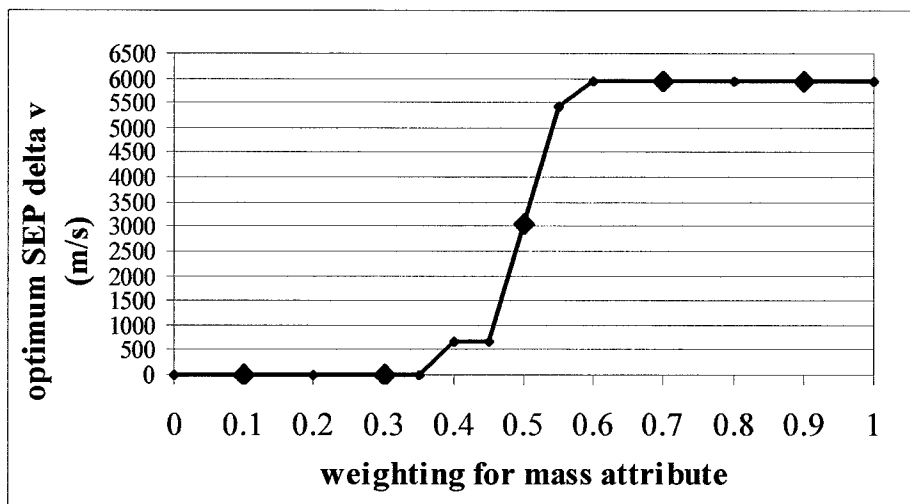
Figure 18. Optimum SEP Δv versus mass attribute weightings (based on results from Figure 17)

In Chapter 4 it was stated that space missions would rarely use linear utility

functions which assume that any increase in the value of an attribute is just as good as an

equivalent decrease is bad (or vice-versa). An assortment of exponential utility functions

was then introduced as a means of more realistically representing utility preferences for

different types of space missions. An example of using these exponential utility functions

is now presented. Suppose that for some specified mission constrained to a specific launch vehicle, the minimum final available mass (700 kg from using total chemical propulsion) is acceptable but limits the mission objectives in some way. However, if 1000 kg of final available mass were achievable, the mission objectives could be met entirely. Any mass available beyond 1000 kg would be beneficial as well, but at a rapidly decreasing rate. We assign the minimum final available mass (700 kg) a zero utility and the maximum final available mass a utility of one. A final available mass of 1000 kg is assigned a value 0.8 utility due to its favorable status. By adjusting the value of R in Eq (7) so that 1000 kg of final available mass yields a utility score of 0.8, the following utility curve was created in Figure 19.
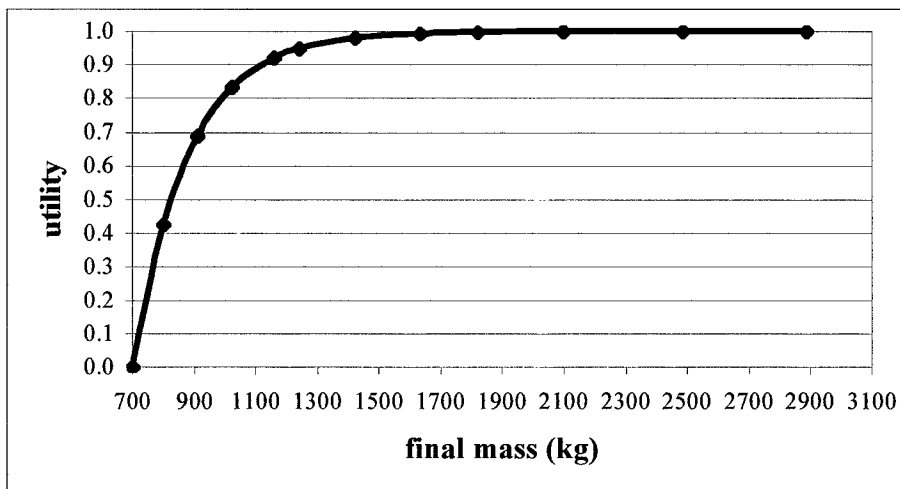
Figure 19. Final available mass utility curve (using Eq (7))

Suppose also the total transfer time required for this mission is somewhat lenient. The spacecraft would normally require several months once in orbit for system testing and verification, and it is decided that a majority of these system checks could be performed

while in a low thrust final orbit transfer. As a result, it is determined that 200 days or less could be allowed for orbit transfer without significantly impacting the mission objectives. Transfer times beyond 200 days (with a maximum of 300 days) could be allowed but quickly become more undesirable with every additional day. A total transfer time of 200 days is assigned a utility value of 0.7 and Eq (5) is used to create the utility curve seen in Figure 20.
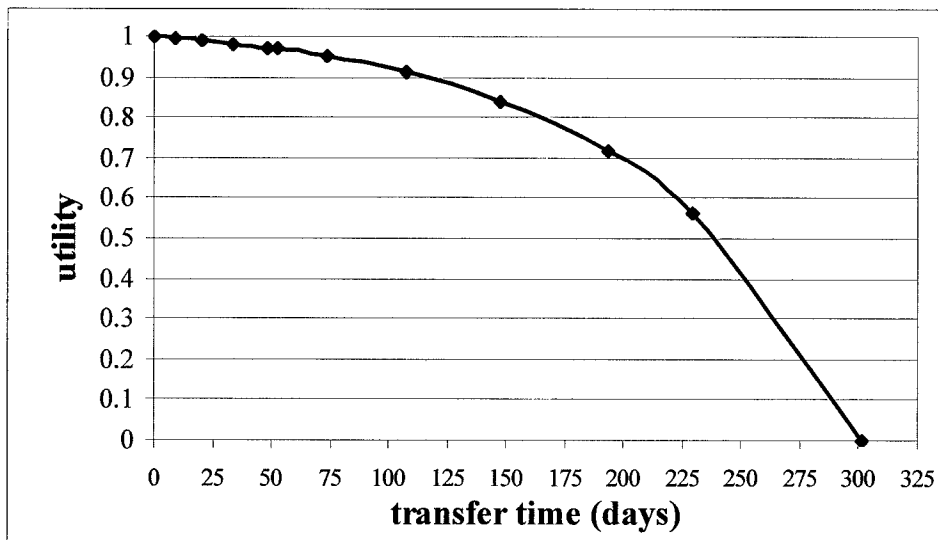
Figure 20. Total transfer time utility curve (using Eq (5))

Following the example from the linear utility functions, Eq (8) is used to combine the exponential utility functions from the mass and time attributes (seen in Figures 19 and 20). This results in a set of total utility functions which is graphed in Figure 21.

41
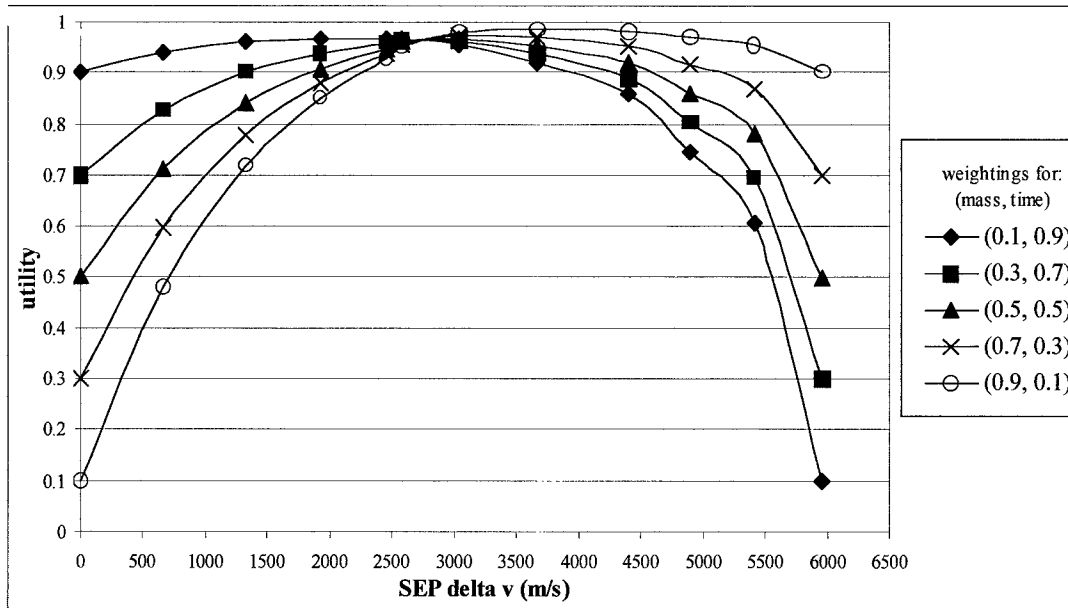
Figure 21. Total utility for orbit transfer (with exponential attributes)

As in the previous example, Figure 21 contains total utility curves for a variety of

weightings of final available mass and total transfer time. Figure 22 contains the optimum

amount of SEP Δv as a function of the mass attribute weightings.
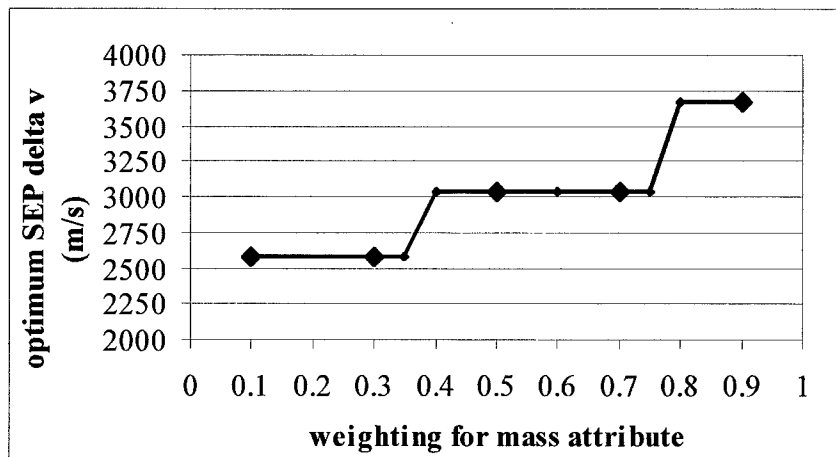
Figure 22. Optimum SEP Δv versus mass attribute weightings (based on results from Figure 21)

42

It is interesting that the optimal orbit insertion strategy, regardless of the weightings selected, requires the use of SEP in combination with either the upper stage alone or the upper stage and an onboard chemical propulsion system. The optimal portion of orbit transfer provided by SEP (represented by the peak of each utility curve) gradually shifts from left to right as the weightings for final available mass increase. This, as expected, represents a gradually increasing use of SEP as the relative importance of final mass is also gradually increased.

Until this point, it has been assumed that the entire range of values for each mission attribute, final available mass and total transfer time, is acceptable for an orbit insertion strategy. Zero utility does not mean unacceptable, and if an unacceptable range of values for final available mass or total transfer time exists, then their utility functions must be constrained. The simplest way to do this is to develop the utility functions as previously explained, but constrain them so they account for only the acceptable regions of attribute values. This will be demonstrated as an example.

For a similar mission as in the previous example, suppose that now a final available mass value less than 1100 kg has been deemed unacceptable due to new requirements. In addition, the spacecraft design has become hungry for available mass and a utility score of 0.5 is given to a final available mass of 2600 kg. Using Eq (6) and substituting 1100 kg as the minimum final mass value (not the minimum final mass value in the range of mass values, which is 700 kg), Figure 23 was constructed. Only the acceptable region of the mass attribute has a utility value between 0 and 1. The rest of its values are unacceptable and not considered.
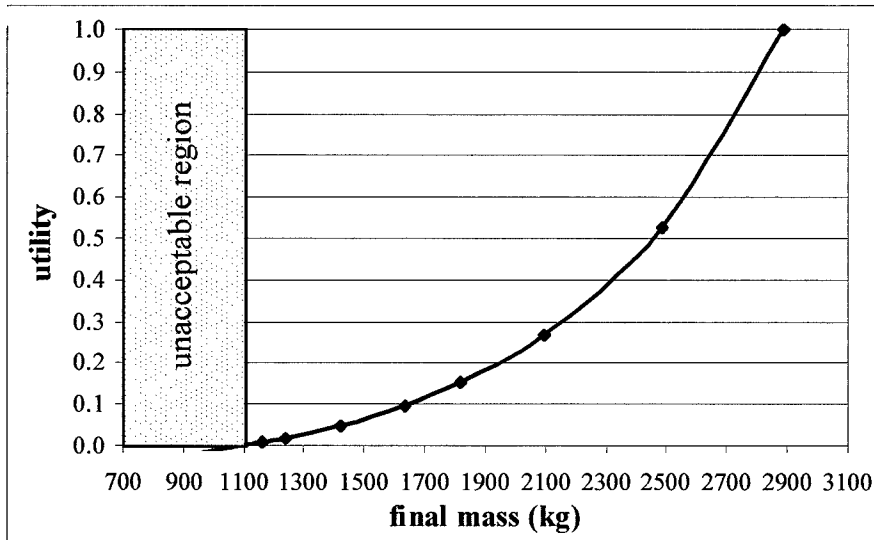
Figure 23. Constrained final available mass utility curve (using Eq (6))

The new requirements for the spacecraft design in this example can no longer have systems checks while in final low thrust orbit transfer; as a result, anything past 200 days is now unacceptable and anything requiring near 200 days for total transfer time will have low utility. A utility value of 0.5 was assigned to 25 days total transfer time and Eq (4) was used to graph the transfer time utility curve in Figure 24.
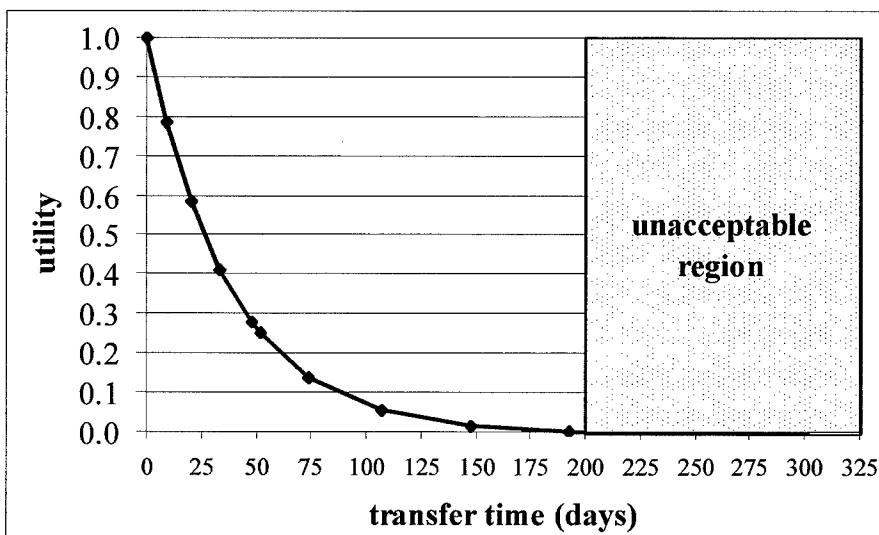
Figure 24. Constrained total transfer time utility curve (using Eq (4))

44

The total utility curve was then constructed from Figures 23 and 24 and again using Eq

(8). It appears as Figure 25 below.
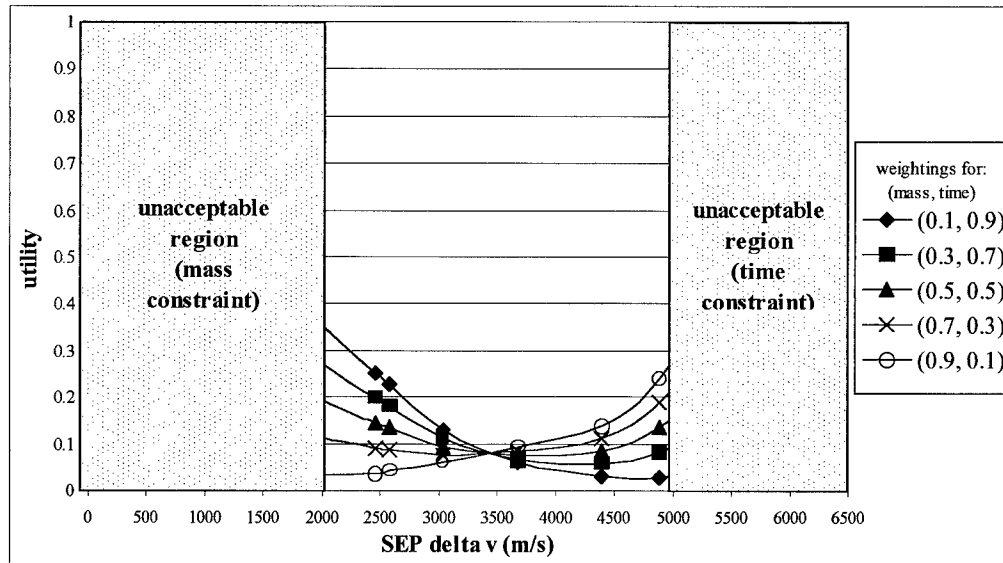
Figure 25. Total utility for orbit transfer (with constrained exponential attributes)

Total utility curves for all weightings in Figure 25 have optimal solutions that require SEP

for partial orbit transfer. This is solely due to the constraints present on both ends of the

graph. Since this example assumed stringent requirements on both final available mass and

total transfer time (while constrained to a specific launch vehicle no less), even the optimal

points have seemingly low utility scores. The highest utility score for all weightings is

only about 0.35. These relatively low utility values for the optimal points do not diminish

the fact that these are the best orbit insertion strategies. Optimal points will simply have

low utility scores when the mission objectives for each attribute conflict severely as in this

example.

Figure 26 shows the amount of SEP Δv that is optimally required for the different mass attribute weightings. It is clear from this graph that mission planners would be in an "either-or" scenario when selecting an optimal orbit insertion strategy, since regardless of the attribute weighting values, only two SEP Δv values are possible as optimal solutions.
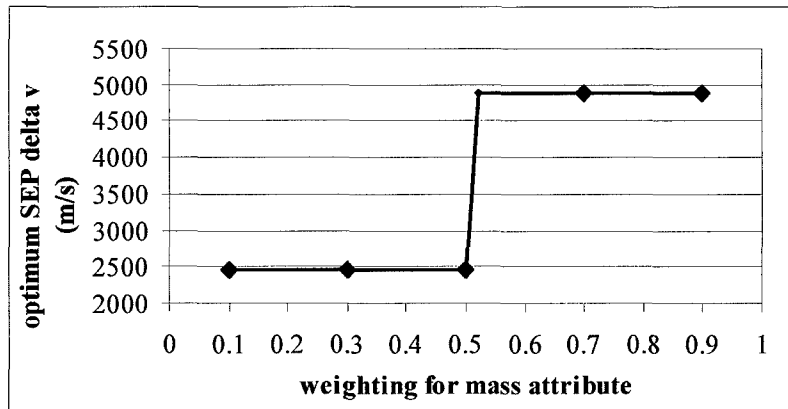
Figure 26. Optimum SEP Δv versus mass attribute weightings (based on results from Figure 25)

This chapter examined the problem of finding an optimal orbit insertion strategy using both chemical and SEP propulsion systems to provide a portion (or all) of orbit transfer to GEO. The launch vehicle specified was not allowed to vary, and the cost associated with the variety of orbit insertion strategies was not considered. Since the cost of orbit insertion could often vary as the orbit insertion strategy is changed, regardless if the launch vehicle does not, this scenario will be examined further in Chapter 5. The launch vehicle specification being constrained is not always an unrealistic assumption, especially due to various political forces at work in the launch community. However, it too will be allowed to vary in the next chapter.

VI. Optimal Orbit Transfer with Constrained Final Available Spacecraft Mass

This chapter will establish a method for finding the optimal combination of high and low-thrust propulsion systems for orbit transfer when the mission is constrained to a final available spacecraft mass. Final available spacecraft mass is defined in section 5.1 and Eq (9). This situation might arise when the spacecraft design mass budget for everything except the on-board propulsion system(s) is nearly frozen and will not change. Since the required launch mass is now a variable (it depends on the orbit insertion strategy employed), launch vehicles are allowed to vary in this chapter. Orbit insertion cost and total transfer time are the two mission attributes that will be traded off to find an optimal solution.

6.1 Cost Assumptions

The major cost driver when estimating the total cost of orbit insertion is the launch vehicle. Often enormous cost savings can be obtained from a single step down in launch vehicle requirements. The launch vehicles considered for use in this effort were in the medium class and consisted of Atlas and Delta launch systems. The launch capacity and cost of each launch system used for this effort is listed in Table 2. The launch cost values were adjusted from FY92$ to FY97$ by using an inflation factor of 1.175 (35:721).

Table 2. Launch system characteristics (10:189, 205)

Launch System	Upper Stage	Max. Payload to LEO (300 km) (kg)	Max. Payload to GTO (kg)	Unit Cost (FY97$M)
Atlas I	Centaur-1	5580	2250	76.375
Atlas II	Centaur-2	6395	2680	82.250
Atlas IIA	Centaur-2A	6760	2810	94.000
Atlas IIAS	Centaur-2A	8390	3490	129.250
Delta II (6920)	PAM-D	3850	1450	52.875
Delta II (7925)	PAM-D	4900	1820	58.750

Estimates for onboard chemical thruster costs and propellant tanks were established from telephone conversations with commercial vendors. A bipropellant thruster assembly was priced at $350K (27). The propellant tanks were priced for various sizes as shown in Figure 27 (9).

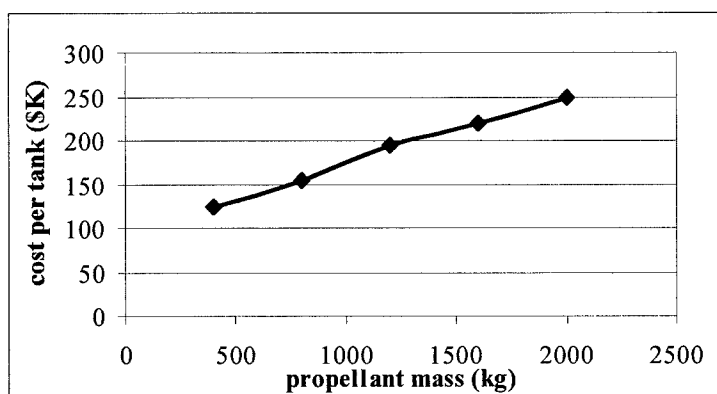Figure 27. Propellant tank costs for on-board bipropellant

Propellant mass values in some cases were below the quantities graphed in Figure 27, so propellant tank cost in these instances were extrapolated. The portion of the SEP xenon propellant tanks required for orbit transfer was also roughly priced using Figure 27. The xenon propellant was priced at $850 per kg while the on-board chemical propulsion

system propellant was not accounted for due to its relative low cost. Additional costs for integrating the two propulsion systems on board the spacecraft were not considered.

Since ground support during the orbit insertion is required for a longer duration when SEP is used, the cost of this support was included and estimated at $18K per day (16:6). Solar panel degradation was also accounted for at the rate of $500 per Watt (16:6).

The equation used in this effort for total orbit insertion cost is displayed as:

$$Cost_{total} = Cost_{launch\ vehicle} + Cost_{chem\text{-}thruster} + Cost_{chem\text{-}tanks} + Cost_{SEP\text{-}tank} + Cost_{xenon} +$$

$$Cost_{ground\ support} + Cost_{power\ degradation} \qquad (10)$$

Each cost quantity in Eq (10) is self-explanatory and follows directly from the explanation above. One point worth noting again, however, is that the quantity $Cost_{SEP\text{-}tank}$ accounts for only the cost of the additional tank volume required for the orbit insertion since the SEP system is assumed to be required for spacecraft orbital maintenance once in operation. The same argument holds for $Cost_{xenon}$, which is only the cost of the xenon propellant required for orbit insertion. Eq (10) is intended to serve only as a rough approximation to the total orbit insertion cost and does not include any integration or development costs which would surely arise for such a mission. These additional costs would need to be included, however, before a truly optimal orbit insertion strategy could be obtained.

6.2 Transfer Time and Cost of Total Orbit Insertion

In this chapter it is assumed that the final available mass of the spacecraft once placed in its final orbit (GEO) will be 1700 kg. A heuristic search method was used with

SEPSPOT to obtain this end condition for each data point since it could not be specified directly within the code. The orbit insertion strategies used here were the same as used in Chapter 5 and explained in section 3.6.

The time required for orbit insertion with the final available mass constrained to 1700 kg (and all other propulsion specifications described in sections 3.3 – 5) is shown as Figure 28.
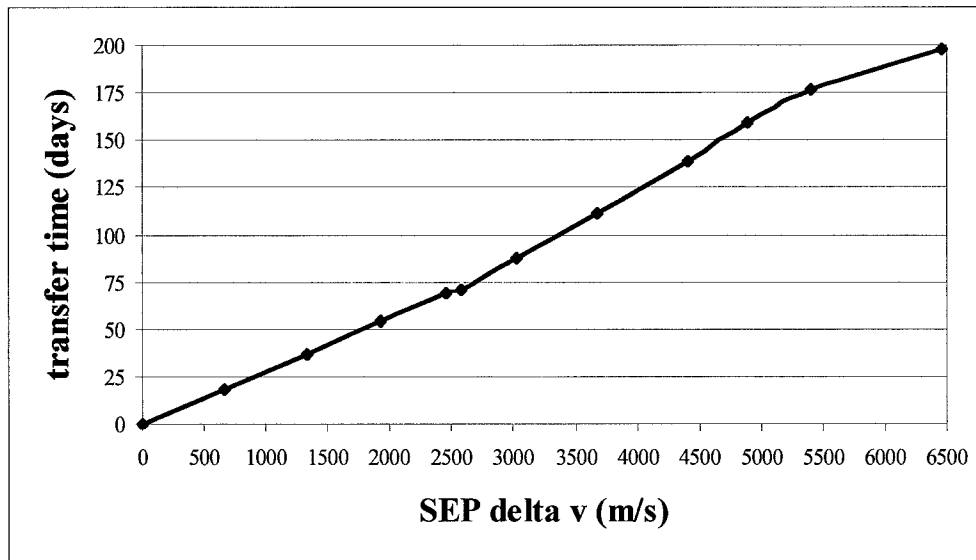
Figure 28. Total transfer time with final available mass constrained at 1700 kg

When compared to the total transfer time graphed in Chapter 5 (Figure 13), which was exponential in shape, Figure 28 appears almost linear. This stems from the final mass constrained to a constant value and the launched mass being allowed to vary. When the launch vehicle was constrained in Chapter 5, the total spacecraft mass at the point in the orbit transfer where the SEP system took over was modeled using the rocket equation (Eq (2)) with Isp values from only chemical propulsion systems. Since the rocket equation is exponential, the initial spacecraft mass at the starting SEP orbit follows an exponential trend which in turn causes the total transfer time calculations to follow an exponential

trend. When the final spacecraft mass is constrained, however, the total spacecraft mass at the point where the SEP system takes over can again be approximated using the rocket equation, but with an Isp value from only the SEP system. This is because we are now working backwards, i.e., using the constrained spacecraft mass at the final orbit and calculating the spacecraft mass at the orbit when the SEP system first took over. The high Isp value for an SEP system minimizes the effects of the exponential term in the rocket equation. The net effect is a total transfer time for the unconstrained launch vehicle case which appears more linear and less exponential than the constrained launch vehicle case.

The total cost of the orbit insertion, using Eq (10) as described above, appears in Figure 29. This figure also shows which launch vehicle was used at each data point on the curve. Table 3 summarizes the insertion strategies used at each of the data points in the figures for this chapter.
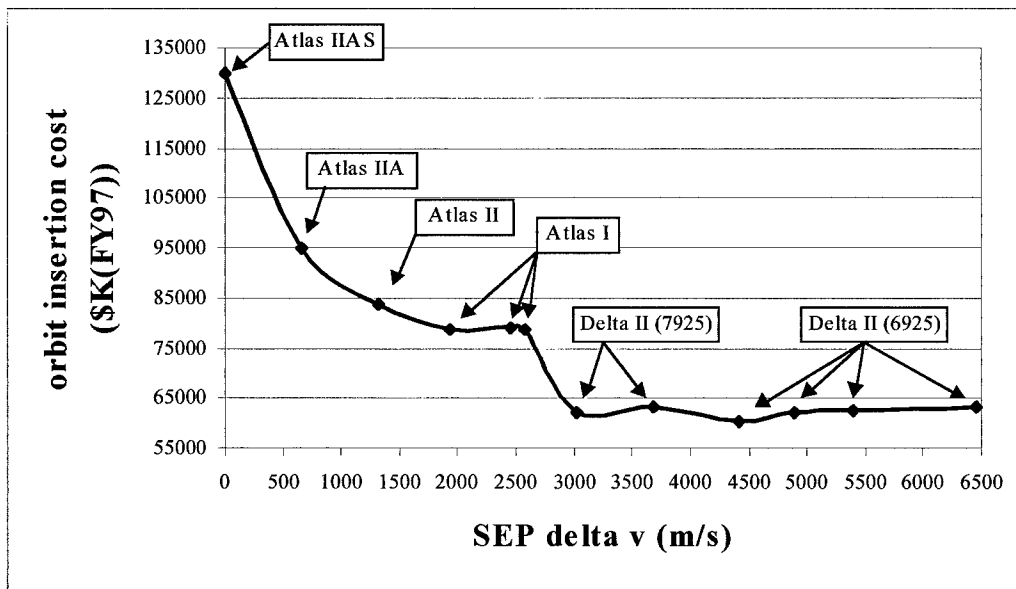

Figure 29. Total cost of orbit insertion with final available mass constrained at 1700 kg

Table 3. Performance calculations for orbit insertion with final available mass fixed at 1700 kg

Orbit insertion strategy	mass after chemical orbit insertion (kg)	launch vehicle required	Electric Propulsion System					Mission Attributes	
			delta v (m/s)	propellant mass (kg)	final mass at GEO (kg)	initial power (kW)	final available mass at GEO (kg)	orbit insertion cost ($K(FY97))	total transfer time (days)
Launch system to GTO, on-board chem. to GEO	1884.0	Atlas IIAS	0	0.0	1884.0	20.0	1834.0	129996	0.0
Launch system to GTO, on-board chemical for some portion, then SEP to GEO	1887.0	Atlas IIA	663	36.1	1850.9	20.1	1794.5	95198	18.6
	1898.0	Atlas II	1324	71.9	1826.2	20.2	1763.5	83809	36.9
	1922.0	Atlas I	1929	105.1	1817.0	21.3	1732.3	78767	54.3
	1933.0	Atlas I	2457	133.6	1799.5	21.7	1704.7	79215	69.5
Launch system to GTO, SEP to GEO	1889.0	Atlas I	2573	136.5	1752.6	22.0	1701.2	78887	70.9
Launch system from LEO (parking orbit) to intermediate orbit between LEO and GTO, then SEP to GEO	1936.0	Delta II (7925)	3019	163.1	1773.0	23.0	1701.3	62099	88.0
	2011.0	Delta II (7925)	3673	204.2	1806.9	24.8	1701.3	63427	111.9
	2151.0	Delta II (6925)	4410	259.5	1891.7	29.6	1699.4	60487	139.0
	2237.0	Delta II (6925)	4896	297.6	1939.6	32.0	1701.1	62134	159.4
	2271.0	Delta II (6925)	5401	330.9	1940.3	31.9	1700.6	62394	177.4
SEP from LEO to GEO	2374.0	Delta II (6925)	6453	407.2	1967.1	32.9	1700.0	63366	198.3

Notice from Figure 29 that the general shape of the total cost curve is exponential with a discrete jump between the Atlas and Delta class launch vehicles. When multiple points on the curve use the same launch vehicle, the curve slopes slightly upward towards increasing cost with increasing SEP Δv. This is due to the increased cost associated with SEP orbit transfer when the launch vehicle is constrained. A more detailed discussion and graph of this effect will be discussed in the next chapter. Notice also that the minimum cost is at the point where the Delta II (6925) is first introduced and requires an SEP orbit transfer with about 4400 m/s Δv. This is a point where the Delta II would launch to an orbit between LEO and GTO and the SEP system would provide the rest of the transfer to GEO (see Table 3).

6.3 Total Utility for Orbit Insertion with Constrained Final Available Spacecraft Mass

Since the final available spacecraft mass is constrained to 1700 kg, the two attributes that vary when we try to find the optimal orbit insertion strategy are total orbit

insertion cost and total transfer time for orbit insertion. The graphs for these two

attributes have already been created in the previous section (Figures 28 and 29) and now

await utility assessment. The maximum total transfer time in this example is under 200

days, which is the duration of time believed by some to be the maximum allowable

transfer time for the vast majority of satellite deployment missions for a transfer to GEO

(31:8). Because of this, a linear utility function was selected for transfer time in this

example, though an exponential utility function (or any other type) could just as easily be

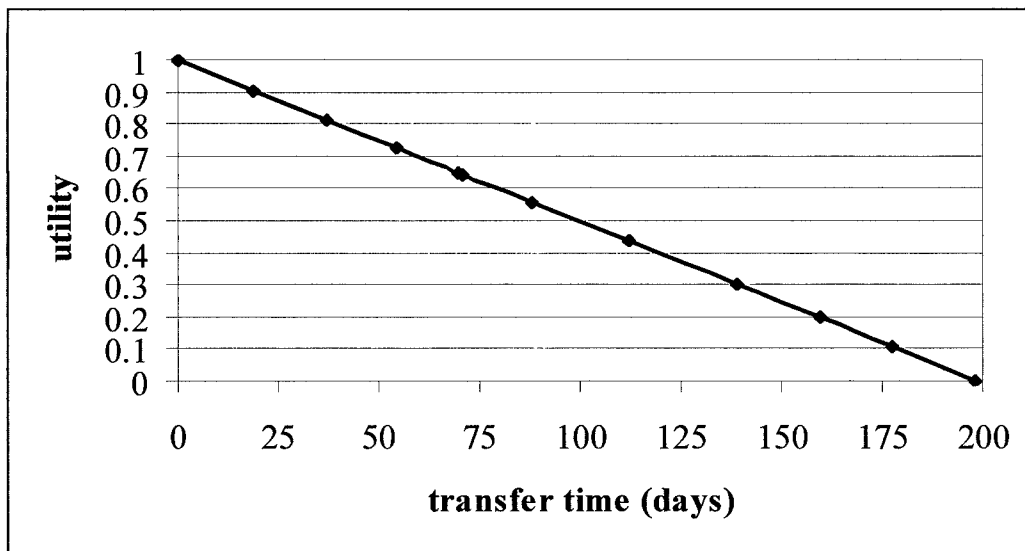applied, as seen in Chapter 5. This utility function appears below as Figure 30.

Figure 30. Total transfer time utility curve (linear with constrained final available mass)

It is also assumed that an increase in cost is just as bad as a decrease in cost of the

same amount is good. Consequently, the total orbit insertion cost can follow a linear

utility curve as well and is seen in Figure 31.

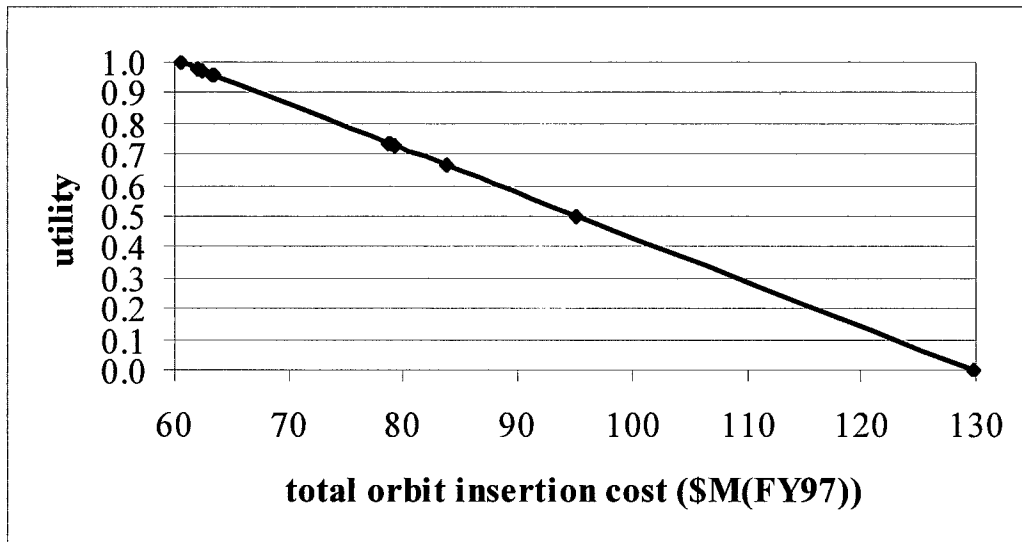Figure 31. Total orbit insertion cost utility curve (constrained final available mass)

The utility functions from the cost and time attributes, as seen in Figures 30 and 31, can be combined using Eq (8) for a total utility expression. This was performed as in the previous chapter and resulted in Figure 32.
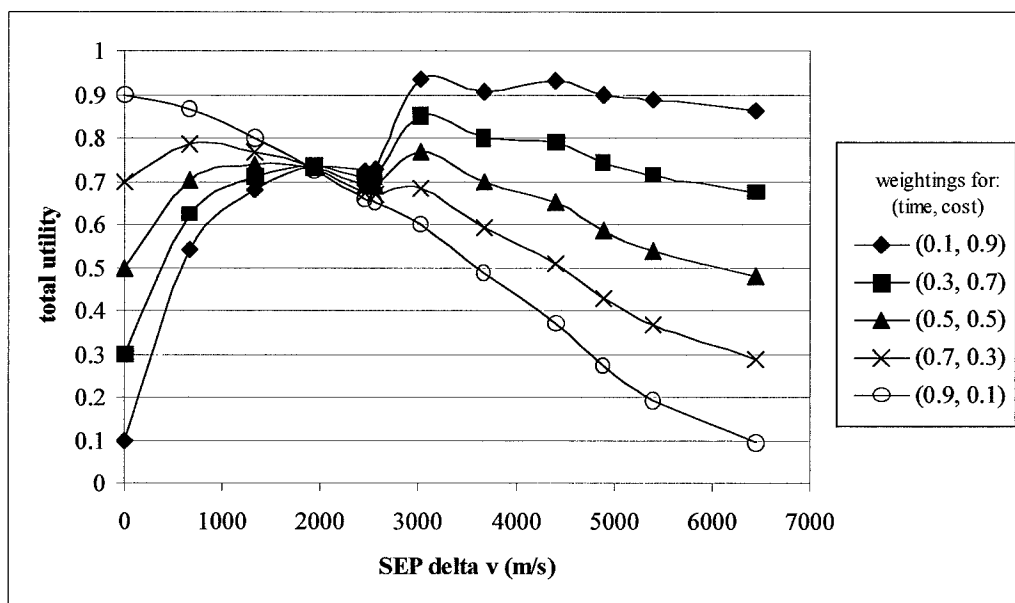

Figure 32. Total orbit insertion utility (linear with constrained final available mass)

54

Figure 32 contains utility curves for a variety of weightings for total transfer time and orbit insertion cost. With the exception of the utility curve most heavily favoring transfer time (which has an optimal orbit insertion strategy using all chemical propulsion), all of the utility curves exhibit optimal solutions which require the use of SEP to provide a portion of the orbit insertion. Figure 33 shows the optimal amount of SEP Δv required for orbit insertion as a function of the weighting used for the transfer time attribute.
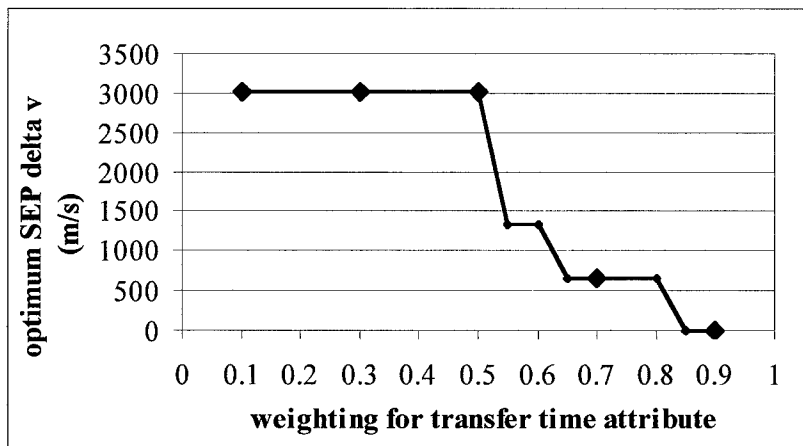
Figure 33. Optimum SEP Δv versus mass attribute weightings (based on results from Figure 32)

It is interesting to note that all of the optimal solutions with weighting schemes that are indifferent or favor cost occur at the same point (roughly at 3000 m/s SEP Δv). By consulting Table 3, it is seen that this point represents the use of a Delta II (7925) launch vehicle to an orbit just less than GTO. At this point the SEP system takes over for the rest of the orbit transfer. This is because all the data points using Delta II class launch vehicles vary very little in orbit insertion cost (notice how level the cost curve becomes for the Delta II class vehicles in Figure 29). Since the minimum orbit insertion cost is in

this region, and for all the Delta II data points, those around 3000 m/s SEP Δv have the local minimum time solution, it becomes apparent why this is the optimal orbit insertion strategy for so many of the weighting schemes. Solutions such as the ones in this example are comforting to mission planners who may know that the attribute weightings for a particular mission will favor cost, but are unsure to what extent. Upon viewing Figures 32 and 33 it becomes apparent that the optimal solution is the same for a wide range of weightings, which adds confidence to the selection of the optimal orbit insertion strategy.

VII. Optimal Orbit Transfer with No Constraints

This chapter describes a method for finding an optimal combination of high and low thrust propulsion systems for orbit transfer when there are no constraints on final spacecraft mass or launch vehicle requirements. This situation might arise early in the space mission planning phase when few spacecraft design parameters have been designated. Finding the optimal combination of high and low thrust propulsion for orbit transfer under these circumstances requires at a minimum the ability to create utility functions for each of the mission attributes and a rough idea of the performance specifications for the onboard chemical and electric propulsion systems. Once the optimal combination of propulsion systems has been established using the method presented in this chapter, mission planners will have a better idea of the orbit insertion cost, transfer time, final available spacecraft mass, and orbit insertion strategy which best suites the mission objectives. This can serve as a basis for further iterations throughout the spacecraft design process.

7.1 Final Mass, Transfer Time, and Orbit Insertion Cost Calculations

The first step towards finding the optimal combination of high and low thrust propulsion systems for an orbit transfer when the final spacecraft mass and launch vehicle are not constrained is to gather a rough idea of the range of final spacecraft masses to be considered. This range of final spacecraft masses will in turn allow the selection of launch vehicles to be considered. An example will be used to demonstrate this process. For this example, the spacecraft's final usable mass delivered to GEO is

required to be in the broad range of roughly 1000 – 4000 kg. Since we now have values

for the range of final spacecraft masses, SEPSPOT and the orbit transfer model (as

described in Chapter 3) can be used with a launch vehicle performance chart (Table 2) to

determine which launch vehicles can be used for this mission. It was found that three

medium class launch vehicles, the Delta II (6925), Delta II (7925), and Atlas I could

provide the range of final spacecraft mass requirements (in combination with a variety of

high and low thrust orbit transfer schemes) and will be considered for this example.

Once the launch vehicles to consider for the mission are specified, calculations

can be made for the spacecraft's final available mass, transfer time, and orbit insertion

cost using each launch vehicle. As in the previous chapters, these calculations can be

conducted as a function of SEP Δv and using a variety of orbit insertion strategies. Since

the launch vehicle is constrained for each set of calculations, the process presented in

Chapter 5 is repeated in this example for each launch vehicle considered.

The first launch vehicle to examine is the Delta II (6925). This was the launch

vehicle previously examined in Chapter 5. Since all of the performance specifications for

the onboard propulsion systems discussed in Chapter 3 are held constant throughout this

effort, the data presented in Chapter 5 for the Delta II (6925) can be used in this example

as well. As with the Delta II (6925) in Chapter 5, SEPSPOT was used to calculate the

optimal combined high and low thrust trajectories for the Delta II (7925) and Atlas I

launch vehicles. . The orbit insertion cost for each launch vehicle was calculated using

Eq (10) from Chapter 6. Graphs of the final available mass, transfer time, and orbit

insertion cost for each of the launch vehicles considered are presented below as Figures
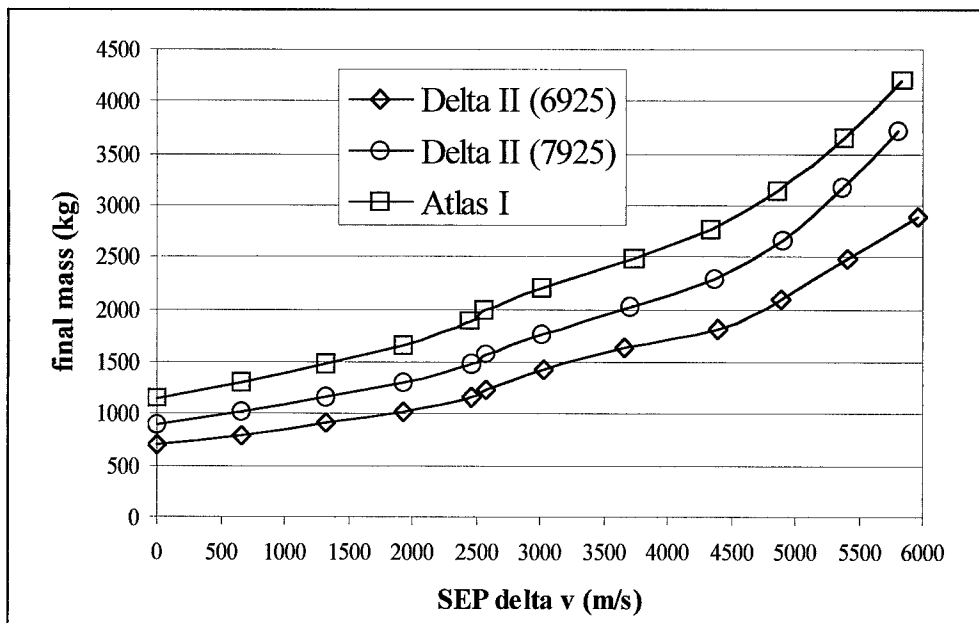
34 – 36.

Figure 34. Final available mass as a function of SEP Δv for three launch vehicles
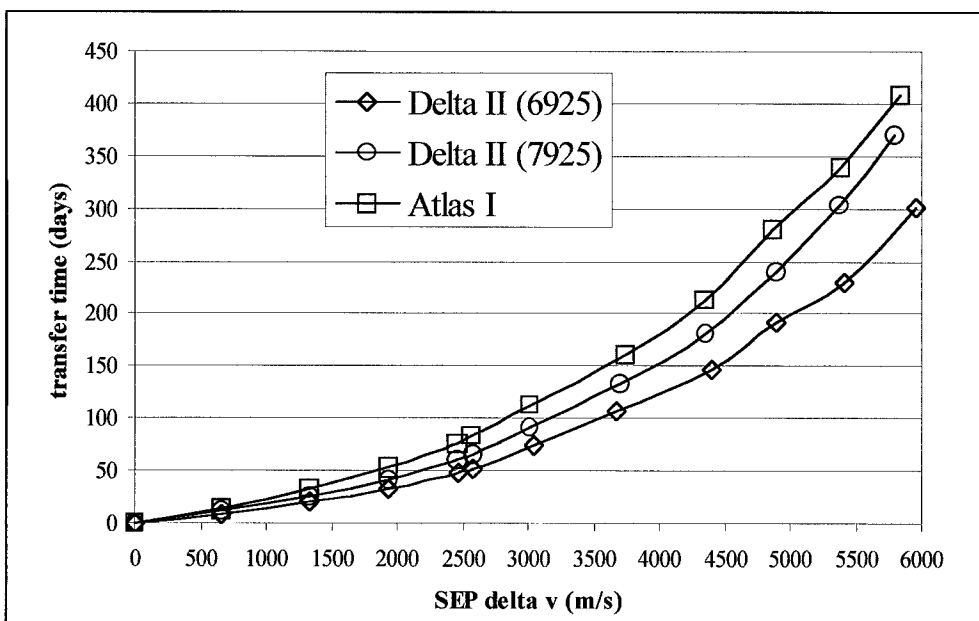

Figure 35. Total transfer time as a function of SEP Δv for three launch vehicles
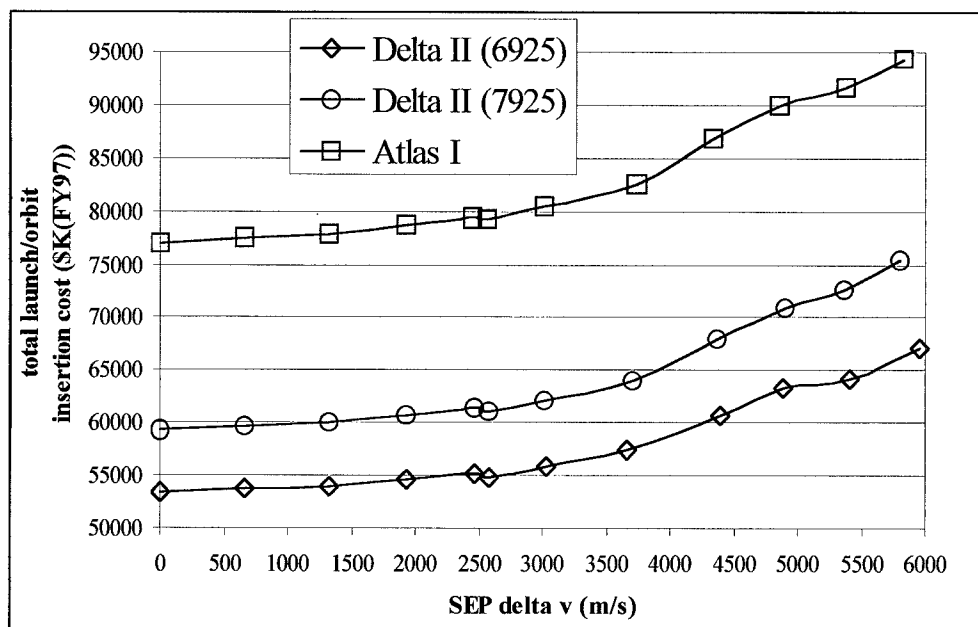
59

Figure 36. Total orbit insertion cost as a function of SEP Δv for three launch vehicles

From viewing Figures 34 – 36 it is easily noticed that the general shape of the curves for each mission attribute (mass, time, and cost) are nearly identical as the launch vehicles vary, while the range of values for each attribute change substantially for different launch vehicles. The curves involving the Delta II (6925) have the lowest range of values for transfer time and orbit insertion cost, but also deliver the lowest range of mass to GEO. The Atlas I delivers the highest range of mass to GEO but also has the highest range of transfer time and cost values. The Delta II (7925) represents a medium range of values for each mission attribute curve. At this point, with such a wide range of attribute values and conflicting preferences, it is apparent that utility analysis must be used to find a preferred launch vehicle and orbit insertion strategy.

Table 4 has been included on the following page to display the data from which Figures 34 – 36 were constructed. Referring to this table will aid the reader in

60

determining the launch strategy used for optimal chemical-SEP system configurations

presented later in this chapter.

Table 4. Performance calculations for orbit insertion with Delta II (6925), Delta II (7925), and Atlas I launch vehicles

launch vehicle	orbit insertion strategy	mass after chemical orbit insertion (kg)	Electric Propulsion System				Mission Attributes		
			delta v (m/s)	propellant mass (kg)	final mass at GEO (kg)	initial power (kW)	final available mass (kg)	total transfer time (days)	orbit insertion cost ($K(FY97))
DELTA II (6925)	Launch system to GTO, on-board chem. to GEO	807.9	0	0.0	807.9	20.0	700.7	0.0	53501.89
	Launch system to GTO, on-board chemical for some portion, then SEP to GEO	917.2	663	17.6	899.6	20.1	800.3	9.1	53783.66
		1041.3	1324	39.4	1001.9	20.1	910.9	20.3	54021.14
		1182.1	1929	64.6	1117.5	20.9	1023.7	33.5	54670.12
		1342.0	2461	92.9	1249.2	21.4	1160.1	48.1	55164.17
	Launch system to GTO, SEP to GEO	1380.0	2576	99.8	1280.2	21.6	1240.3	52.1	54809.17
	Launch system from LEO (parking orbit) to intermediate orbit between LEO and GTO, then SEP to GEO	1624.7	3035	137.5	1487.7	22.8	1423.0	73.9	55836.55
		1930.7	3669	195.7	1735.3	24.7	1632.7	107.5	57410.40
		2294.3	4398	275.9	2019.0	29.9	1819.5	147.7	60813.44
		2726.4	4892	362.2	2363.9	33.2	2097.7	192.9	63377.11
		3239.8	5415	472.9	2767.1	33.4	2483.8	229.4	64216.84
	SEP from LEO to GEO	3850.0	5958	613.5	3236.5	36.3	2886.2	301.6	67116.96
DELTA II (7925)	Launch system to GTO, on-board chem. to GEO	1024.5	0	0.0	1024.5	20.0	902.0	0.0	59400.86
	Launch system to GTO, on-board chemical for some portion, then SEP to GEO	1163.1	663	22.3	1140.7	20.1	1028.1	11.5	59730.61
		1320.5	1324	50.0	1270.1	20.1	1168.3	25.7	60027.34
		1499.1	1930	82.0	1417.0	21.1	1313.3	42.4	60799.74
		1701.9	2459	117.7	1584.3	21.5	1488.8	61.2	61364.58
	Launch system to GTO, SEP to GEO	1750.0	2575	126.5	1623.5	21.8	1576.7	66.1	61065.96
	Launch system from LEO (parking orbit) to intermediate orbit between LEO and GTO, then SEP to GEO	2009.7	3016	169.1	1840.9	23.1	1767.8	91.5	62187.68
		2401.8	3703	245.7	2156.3	25.3	2036.9	132.7	64095.36
		2870.5	4359	342.4	2527.7	31.2	2297.8	181.4	68011.73
		3430.6	4896	456.1	2974.9	34.7	2671.9	240.8	70941.43
		4100.0	5370	593.8	3506.2	35.7	3167.9	303.2	72717.49
	SEP from LEO to GEO	4900.0	5800	761.9	4138.2	38.5	3732.1	370.3	75466.27
ATLAS 1	Launch system to GTO, on-board chem. to GEO	1288.0	0	0.0	1288.0	20.0	1146.8	0.0	77055.00
	Launch system to GTO, on-board chemical for some portion, then SEP to GEO	1462.2	663	28.0	1434.0	20.1	1305.4	14.4	77441.71
		1660.0	1324	62.8	1597.2	20.2	1482.2	32.3	77815.32
		1884.6	1929	103.0	1782.0	21.2	1666.5	53.3	78730.52
		2139.5	2456	147.8	1991.3	21.7	1887.3	76.4	79393.04
	Launch system to GTO, SEP to GEO	2200.0	2557	157.9	2042.1	22.1	1986.5	83.6	79175.13
	Launch system from LEO (parking orbit) to intermediate orbit between LEO and GTO, then SEP to GEO	2496.0	3015	209.9	2286.1	23.5	2201.0	113.2	80441.19
		2923.3	3739	301.8	2621.3	25.9	2483.5	160.5	82607.83
		3423.7	4338	406.5	3017.5	32.2	2762.3	213.7	86787.66
		4009.7	4862	529.7	3480.3	36.1	3144.5	280.6	90051.14
		4696.1	5384	681.8	4014.3	36.9	3645.6	340.0	91656.53
	SEP from LEO to GEO	5500.0	5835	859.8	4640.2	39.3	4208.0	408.8	94275.20

7.2 Establishing Utility for Mission Attributes

In the previous section the range of final spacecraft masses to be considered was used to specify the candidate launch vehicles. For each launch vehicle considered, the range of values for final usable mass, transfer time, and orbit insertion cost was calculated (Figures 34 – 36). The utility functions for each mission attribute must now be determined. Since the range of values for final available mass, transfer time, and orbit insertion cost are now all known, analysis can be conducted using these values to establish utility functions for each attribute.

The initial range of final spacecraft mass values for this example mission was selected as roughly between 1000 and 4000 kg at the beginning of section 7.1. After running the SEPSPOT computer code with performance values from the three specified launch vehicles, the entire range of final spacecraft mass values (achievable with the three launch vehicles) was calculated to range from 700 to 4200 kg (as seen in Figure 34). Since the range of acceptable final mass values was only a crude estimate, the latter range of final spacecraft mass values was deemed acceptable for this mission. As a result, the utility function for final usable spacecraft mass must have a zero utility score for 700 kg and a utility score of one for 4200 kg. A final available mass of 2000 kg was chosen by the mission planner to have a utility score of 0.8 in this example after an exponential utility function was selected (Eq (7)). Figure 37 shows the resulting utility function for the final available mass.
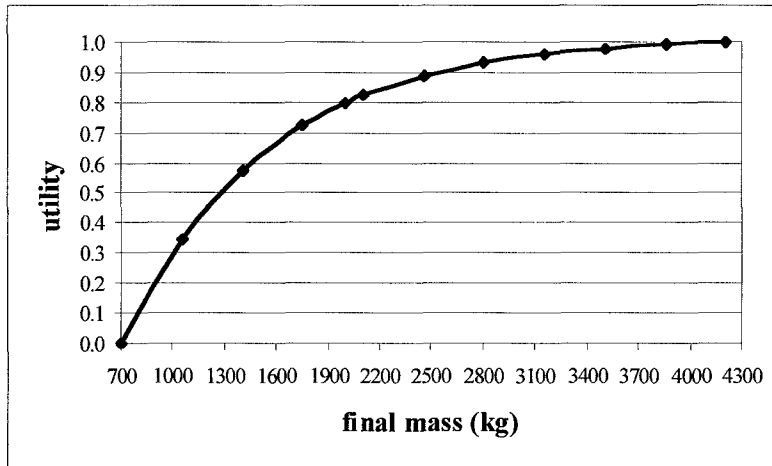
Figure 37. Final available mass utility curve

Figure 37 represents the utility function for the entire spectrum of possible final available masses from any of the three launch vehicles. This utility function was then used to calculate the utility scores for final available mass delivered using each of the three launch vehicles separately. Graphs of the results are shown in Figures 38 – 40.
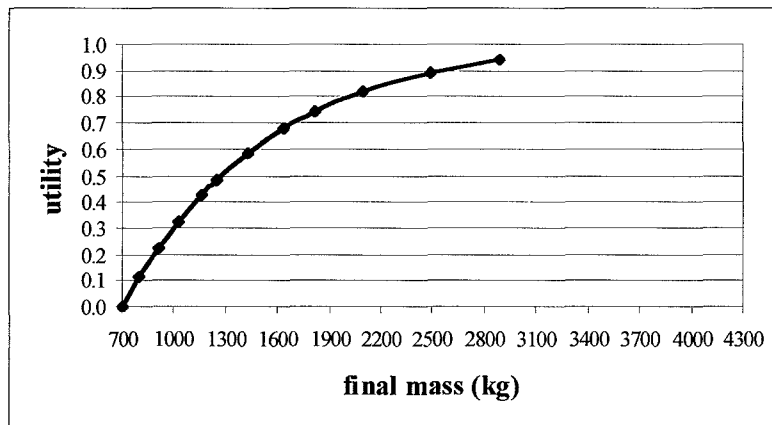

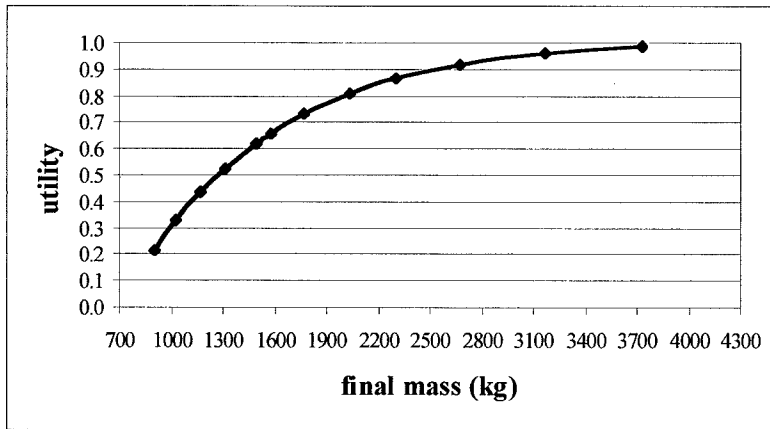Figure 38. Final available mass utility curve for Delta II (6925)

Figure 39. Final available mass utility curve for Delta II (7925)
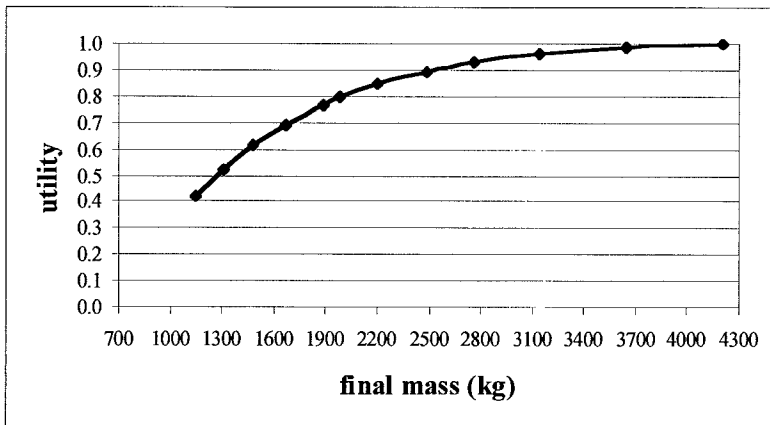
Figure 40. Final available mass utility curve for Atlas I

Notice that none of the graphs in Figures 38 – 40 range between utility scores of zero and one when viewed separately, but together they represent the utility function shown in Figure 37.

The same process was next applied to the orbit transfer time attribute. The most preferred transfer time was zero days (all chemical propulsion transfer) and obtainable using any launch vehicle. The longest transfer time was 409 days using the Atlas I launch vehicle and an all SEP LEO-to-GEO transfer. The mission objectives for this

64

example cannot allow transfer times to exceed 250 days due to mission related time

constraints. As a result, the time attribute utility function assigned a zero utility score to a

transfer time value of 250 days. The mission planner assigned a transfer time requiring

225 days a utility score of 0.4 and the graph in Figure 41 displays the resulting
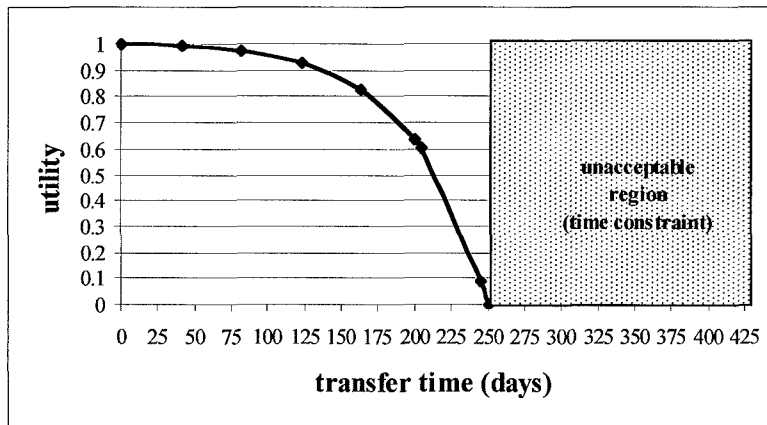
exponential utility function of the form of Eq (5).

Figure 41. Total transfer time utility curve

The utility curves for transfer time for each of the launch vehicles are next shown in
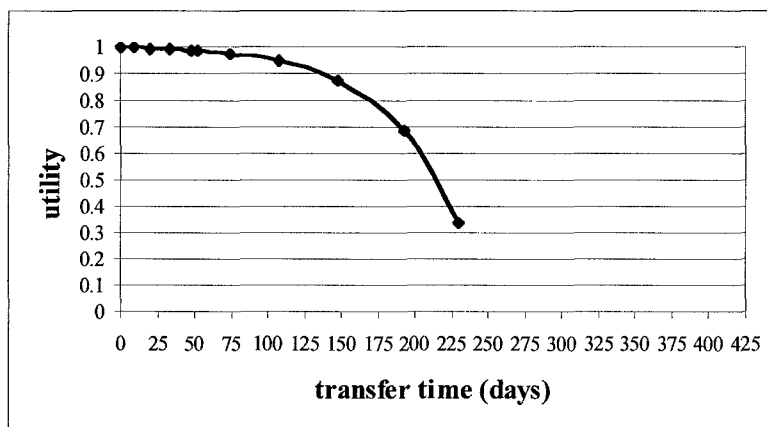
Figures 42 – 44.

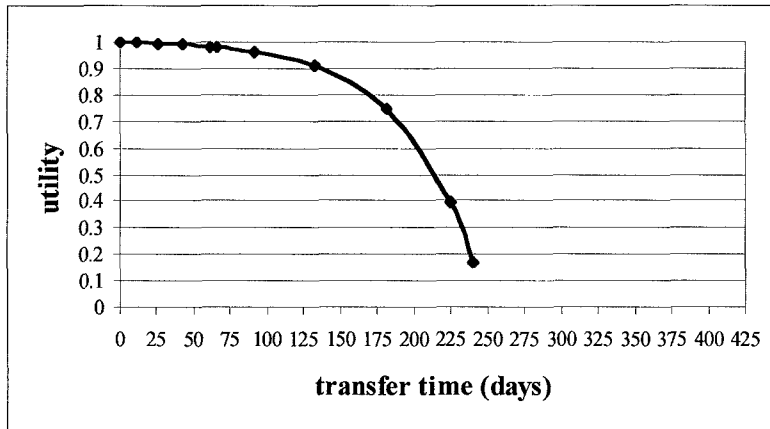**Figure 42. Total transfer time utility curve for Delta II (6925)**

65

Figure 43. Total transfer time utility curve for Delta II (7925)
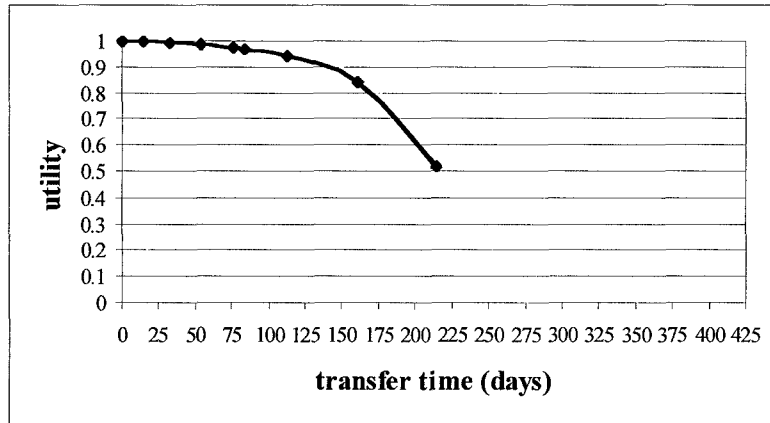

Figure 44. Total transfer time utility curve for Atlas I

A linear utility function for orbit insertion cost was selected by the mission planner as representative of the cost preferences for this mission. This, as previously mentioned, views a decrease in the cost of orbit insertion by a specified amount as favorable as an increase in cost by the same amount would be unfavorable. The total orbit insertion cost utility function is graphed in Figure 45.
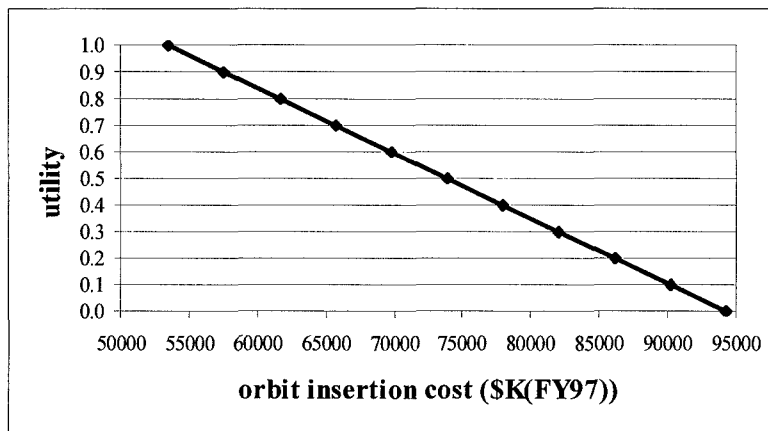
66

Figure 45. Total orbit insertion cost utility curve

The orbit insertion cost utility curves for each of the launch vehicles follow in Figures 46 – 48.
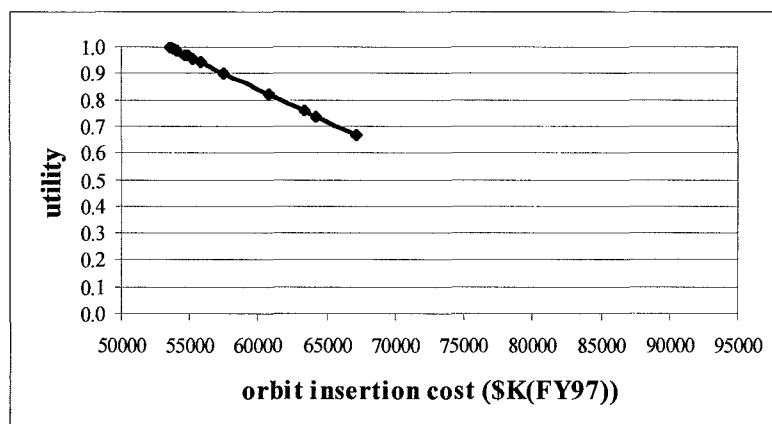

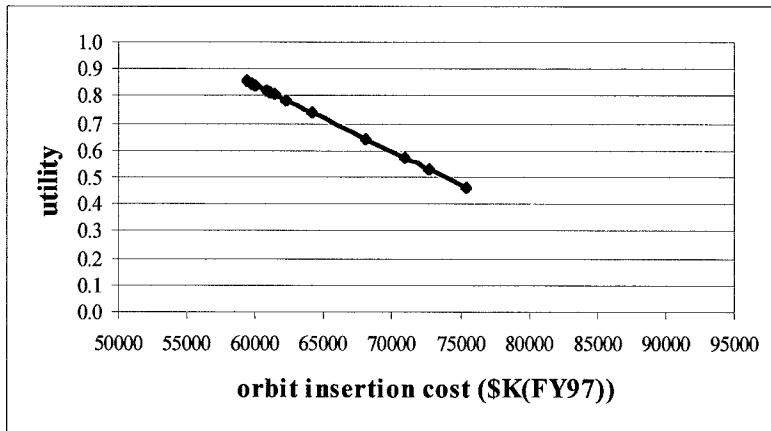**Figure 46. Total orbit insertion cost utility curve for Delta II (6925)**

67

Figure 47. Total orbit insertion cost utility curve for Delta II (7925)
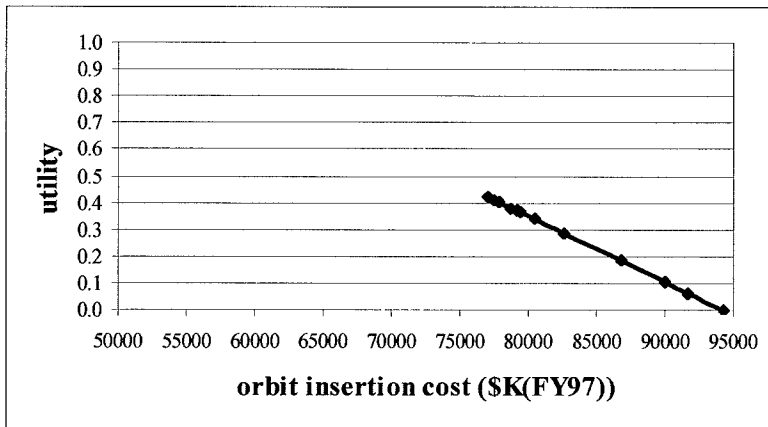

Figure 48. Total orbit insertion cost utility curve for Atlas I

As with the previous attribute utility curves, each launch vehicle's total orbit insertion cost utility makes up a portion of the total cost utility curve for the mission. Using this approach will allow us to compare total mission utility scores for each launch vehicle as we attempt to find the optimum orbit insertion strategy.

7.3 Total Mission Utility

At this point we now have utility functions for each mission attribute (mass, time, and cost) for each launch vehicle considered. This is enough information required to find the optimal orbit insertion strategy for the mission. To accomplish this, we must compare the total utility scores of each launch vehicle as the portion of the orbit transfer provided by SEP is varied, with the highest utility score representing the overall optimum orbit insertion strategy. The total utility score can be computed by using Eq (8) with acceptable preference weightings for each of the mission attributes.

Figures 49 – 54 show the total utility scores for the orbit insertion of the spacecraft in this example as a function of SEP Δv for each of the launch vehicles considered. These graphs were constructed from the data shown in Figures 34 – 48. A variety of weightings were used in constructing these graphs in order to represent a diversity of preferences toward final available spacecraft mass, total transfer time, and total orbit insertion cost.
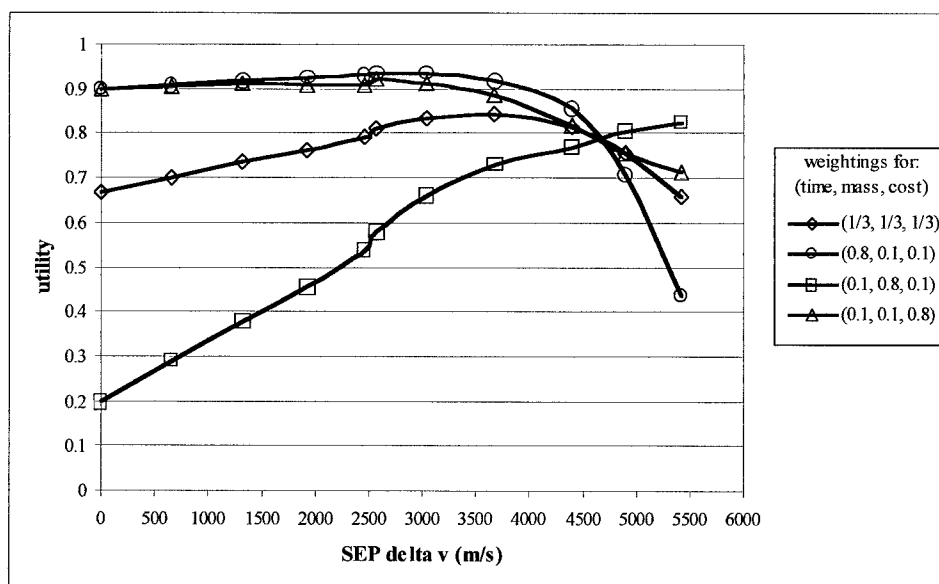

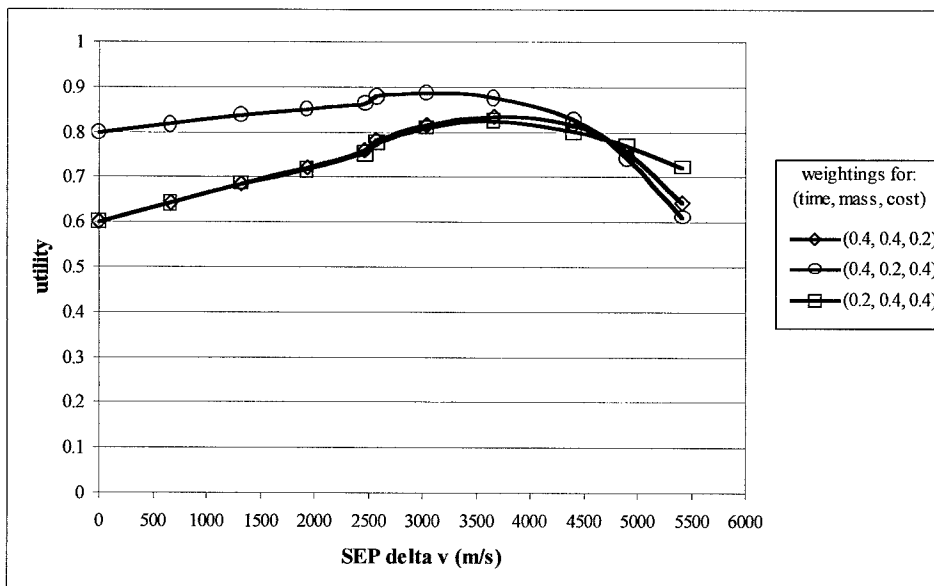**Figure 49. Total orbit insertion utility using Delta II (6925) [part 1]**

69

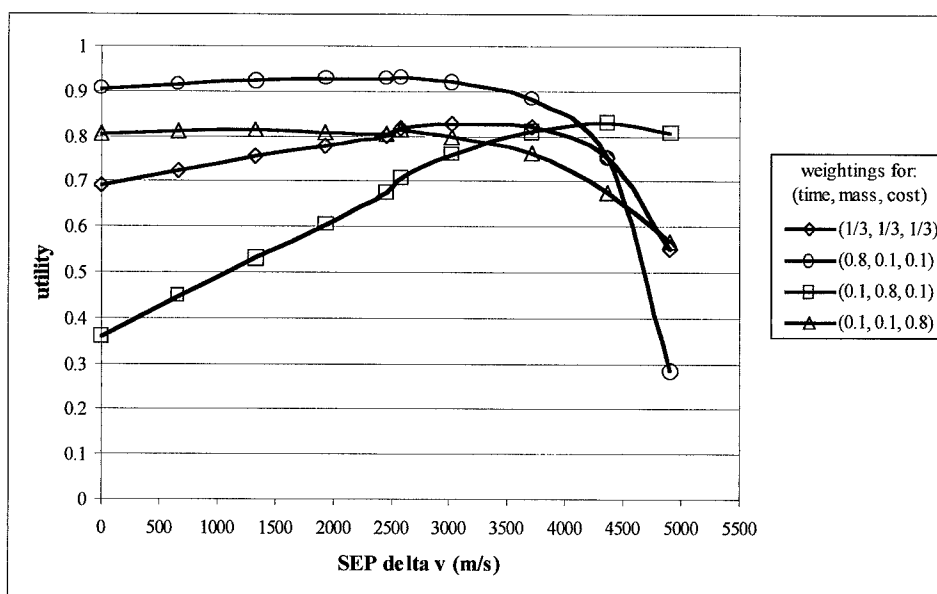**Figure 50. Total orbit insertion utility using Delta II (6925) [part 2]**

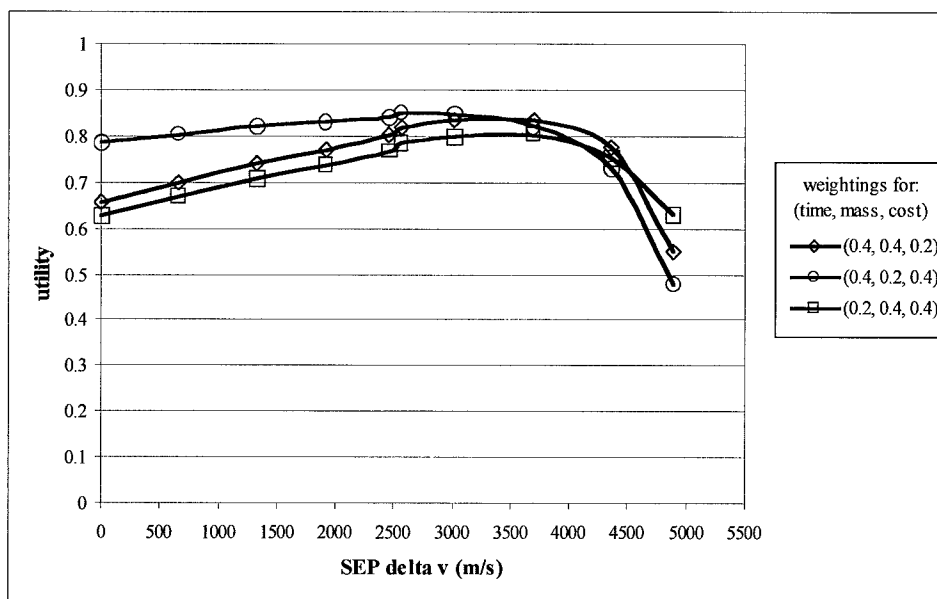**Figure 51. Total orbit insertion utility using Delta II (7925) [part 1]**

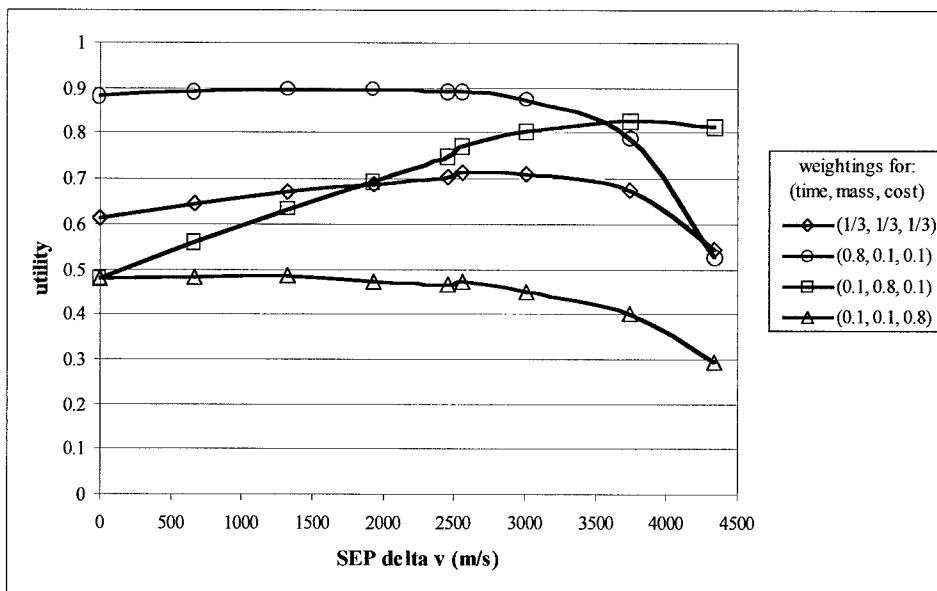**Figure 52. Total orbit insertion utility using Delta II (7925) [part 2]**

Figure 53. Total orbit insertion utility using Atlas I [part 1]
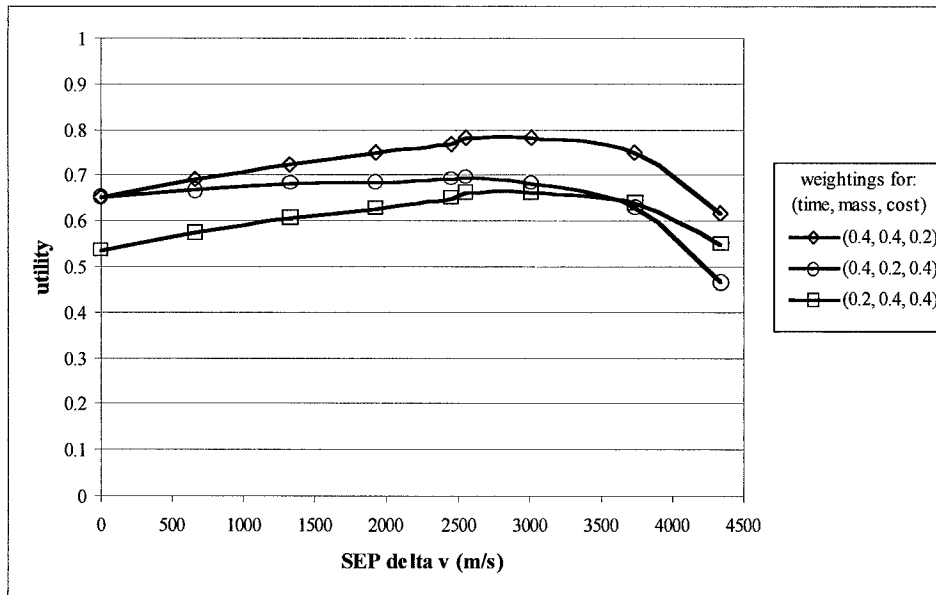
71

Figure 54. Total orbit insertion utility using Atlas I [part 2]

For almost all of the curves in Figures 49 – 54, the optimum orbit insertion strategy involved using SEP for a portion of the orbit transfer. In fact, none of the orbit insertion scenarios required an all chemical transfer and only one case required an all SEP orbit transfer (the Delta II (6925) did when the mass attribute was heavily favored).

While viewing the total utility curves from Figures 49 – 54 make it easy find the optimal orbit insertion strategy for each launch vehicle considered, the utility curves should be grouped differently to find the optimal orbit insertion strategy for the overall mission. Figures 55 – 61 provide such a grouping. There are three curves in each figure representing total utility functions from each of the launch vehicles considered. Each figure represents a specific weighting of mission attributes used in Eq (8) to compute the total utility score. Although each curve will have a local maximum representing the optimum orbit insertion strategy when using that particular launch vehicle, one of these curves will have a point with the highest utility score of all curves considered. The point

72

along the curve where that value exists represents the optimum orbit insertion strategy for the mission given that figure's particular attribute weighting scheme.

Figure 55. Total orbit insertion utility for the example mission with attribute weighting scheme of: (time, mass, cost) = (1/3, 1/3, 1/3)

Figure 56. Total orbit insertion utility for the example mission with attribute weighting scheme of: (time, mass, cost) = (0.4, 0.4, 0.2)

Figure 57. Total orbit insertion utility for the example mission with attribute weighting scheme of: (time, mass, cost) = (0.4, 0.2, 0.4)

Figure 58. Total orbit insertion utility for the example mission with attribute weighting scheme of: (time, mass, cost) = (0.2, 0.4, 0.4)

Figure 59. Total orbit insertion utility for the example mission with attribute weighting scheme of: (time, mass, cost) = (0.8, 0.1, 0.1)

Figure 60. Total orbit insertion utility for the example mission with attribute weighting scheme of: (time, mass, cost) = (0.1, 0.8, 0.1)
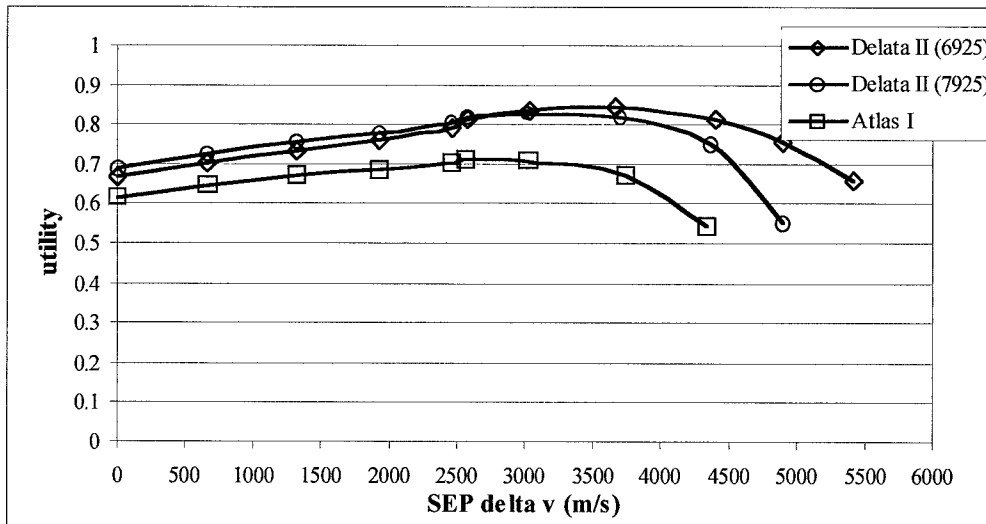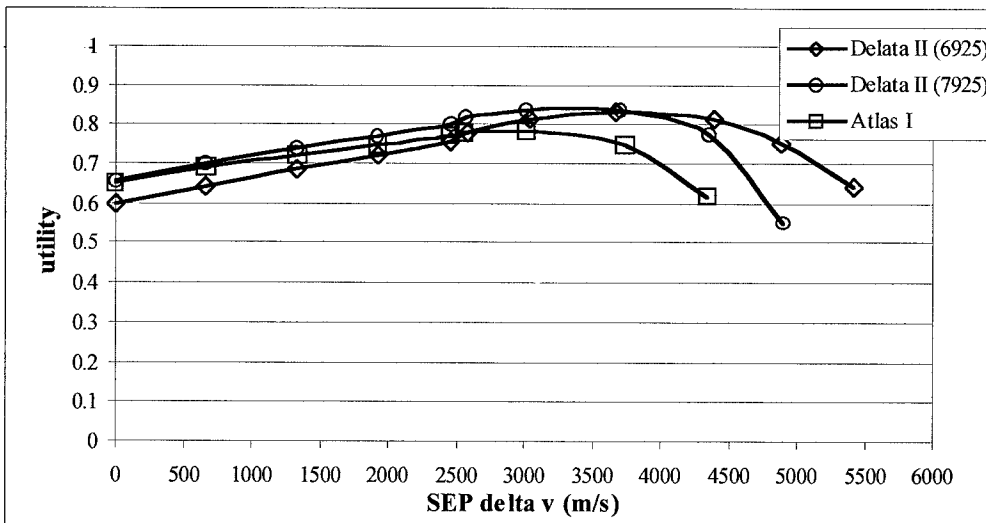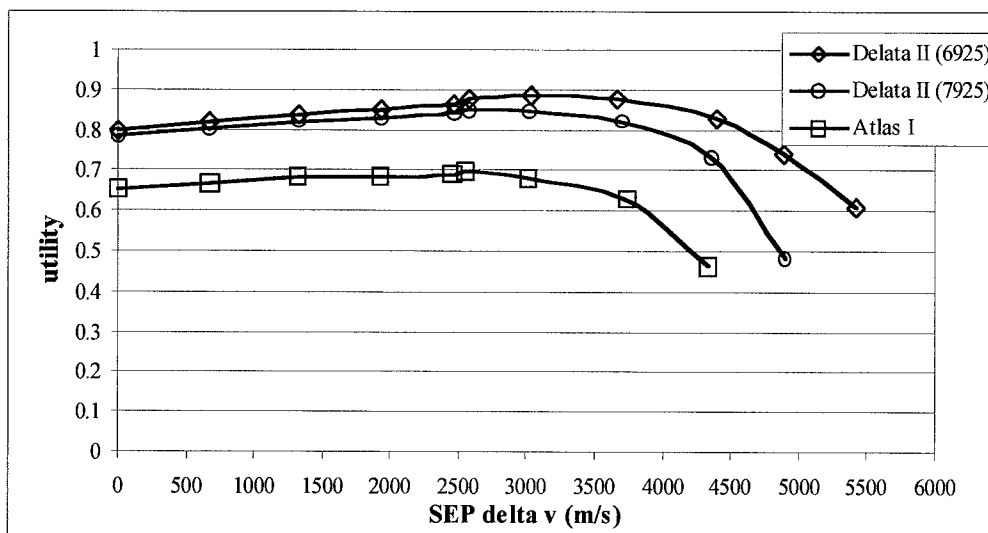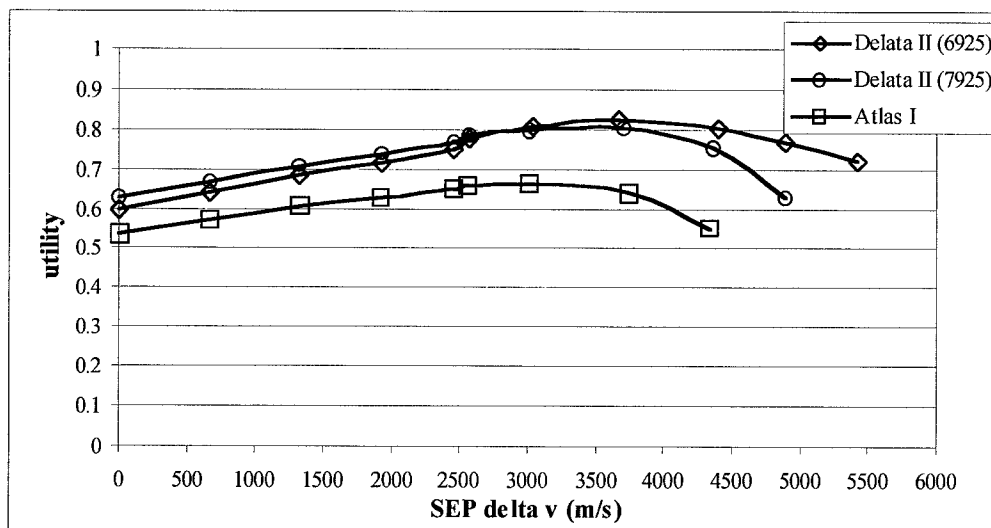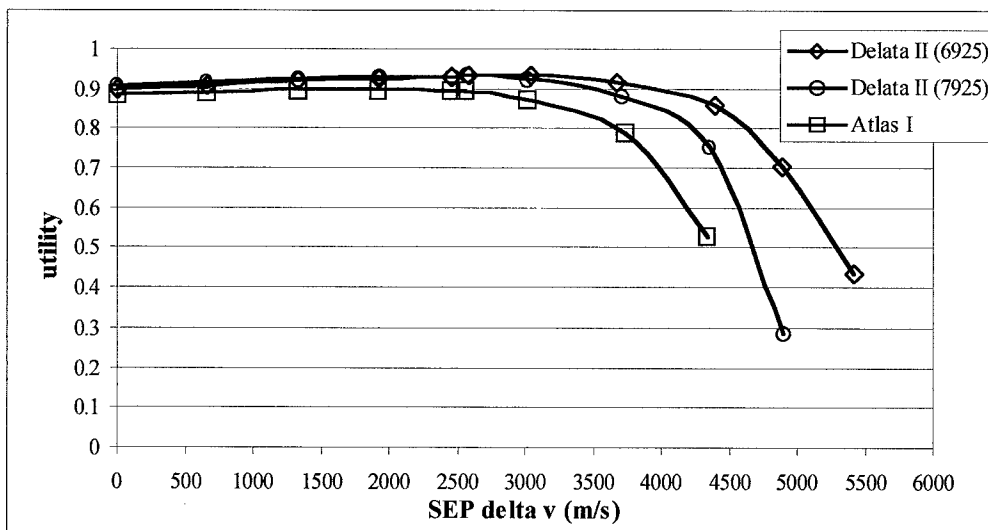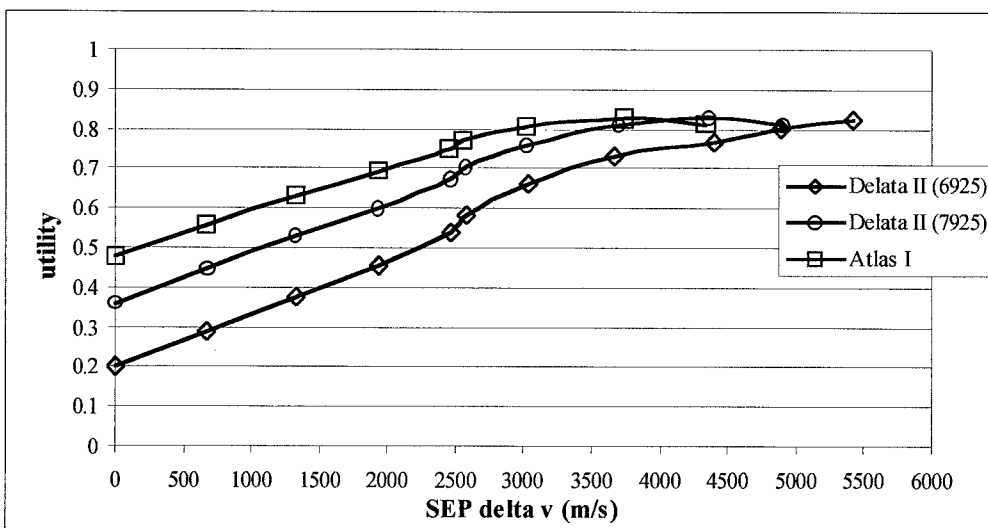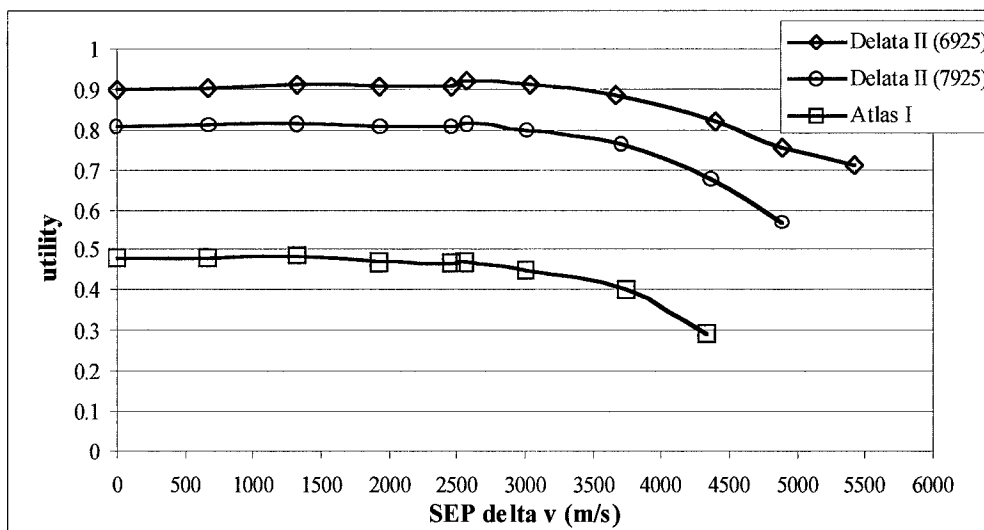
Figure 61. Total orbit insertion utility for the example mission with attribute weighting scheme of: (time, mass, cost) = (0.1, 0.1, 0.8)

Figure 62 below summarizes the maximum utility scores for each launch vehicle from Figures 55 – 61.
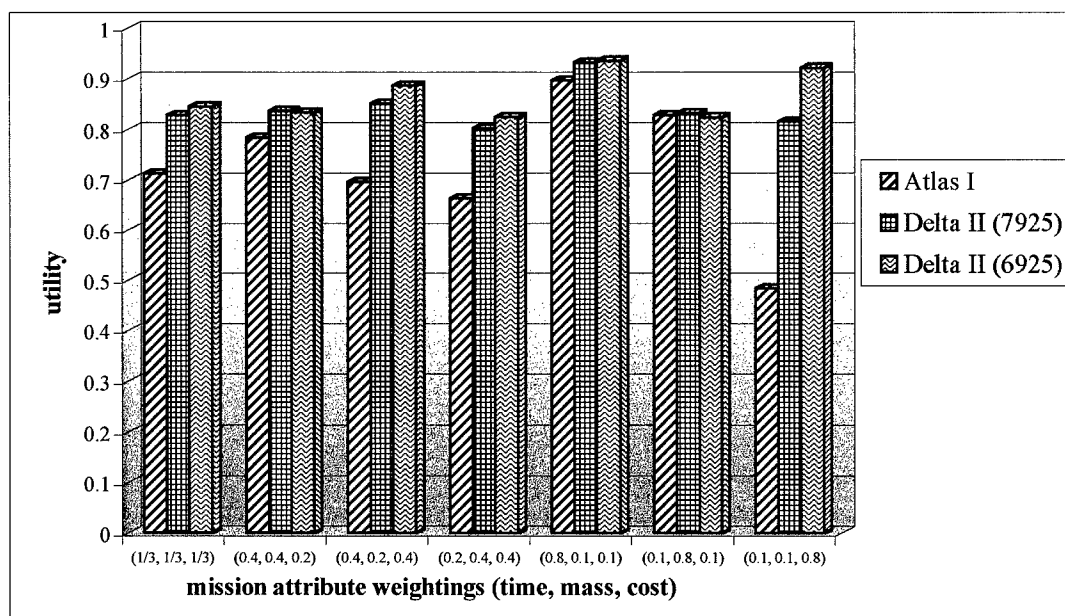
Figure 62. Highest utility score for each utility curve in Figures 55-61

Figure 63 shows the optimal amount of SEP Δv required for orbit insertion as a function of the weightings used for the final available mass and transfer time attributes. This figure can be used to see general trends in how the optimal amount of SEP Δv required for orbit insertion relates to the mission attribute weightings.
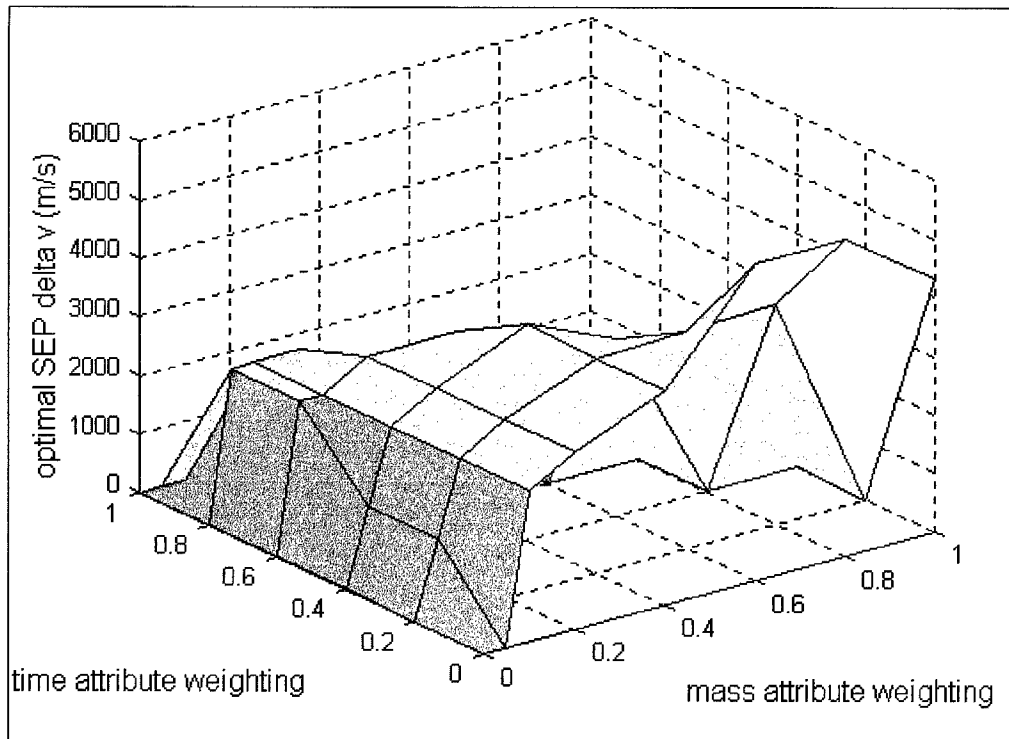
Figure 63. Optimum SEP Δv versus mass and time attribute weightings (based on results from Figure 55 - 61)

From viewing Figures 55 – 63 and using Table 4, the optimal orbit insertion strategy for the example mission can be found for each of the attribute weighting schemes presented. For the attribute utility functions and attribute weighting schemes used in this example, it is interesting to note that none of the optimal orbit insertion strategies require the use of the Atlas I launch vehicle and few require the use of a chemical propulsion system onboard the spacecraft. Upon examining the attribute utility functions used for

this example the reason becomes apparent. The range of values for orbit insertion costs and transfer times are both lower for the Delta II class launch vehicles. Transfer times are lower because the smaller launch vehicles launch less mass, thus it requires less time for the SEP portions of the orbit transfer. The Delta II class launch vehicles receive notably higher utility scores for both the cost and time attributes when compared to the Atlas I launch vehicle for any given orbit insertion strategy. The Atlas I has the advantage over the Delta II class launch vehicles for the range of values for final available spacecraft mass, but the exponential shape of the mass utility function (Figure 37) gives nearly equally high utility scores for a broad range of large mass values and the transfer time constraint eliminates some of the larger mass values from consideration. As a result, the maximum utility scores obtainable by the Atlas I for the mass attribute are only slightly higher than the maximum utility scores obtainable by either of the Delta II launch vehicles. The Atlas I can therefore not compete with the total utility scores from the Delta II vehicles.

The reason for the absence of an onboard chemical propulsion system in nearly all of the optimal orbit insertion strategies is more difficult to see immediately. Any orbit insertion strategy which requires the SEP system to begin its portion of an orbit transfer from beyond a GTO starting orbit will require an onboard chemical propulsion system (see Chapter 3). All of the higher mass utility scores are available at SEP starting orbits at or before GTO. SEP starting orbits beyond GTO are in the region of the exponential mass utility curve (Figure 37) where utility scores rapidly diminish as more and more of the onboard chemical propulsion system is used. Conversely, the cost and time utility curves increase the utility score as more of the onboard chemical propulsion system is

used, but not at as steep a rate as the mass utility decreases. As a result, the best opportunity for an optimum orbit insertion strategy requiring an onboard chemical propulsion system in this example occurs when both the time and cost attributes are considerably more important than mass. Figure 57 seems to fit this requirement with an attribute weighting scheme of 0.4, 0.2, 0.4 for time, mass, and cost respectively, but it is not slanted quite enough in favor of time and cost. Had an additional figure been included with an attribute weighting scheme of 0.45, 0.1, 0.45 for time, mass, and cost respectively, an optimum orbit insertion strategy requiring onboard chemical propulsion would have resulted. This can be seen on Figure 63 as well.

This chapter showed by example how an optimal orbit insertion strategy using both chemical propulsion and SEP systems can be derived when neither the launch vehicle nor final spacecraft mass is constrained. This would typically occur early in the space mission planning phase. The optimal orbit insertion strategy calculated using the method in this chapter would typically serve as a baseline approach. Further iterations could later be conducted as the spacecraft design becomes better defined, possibly using the methods presented in Chapters 5 or 6.

VIII. Conclusions

This effort presented a method for finding the optimal portion of an orbit transfer to be provided by a low thrusting solar electric propulsion system in place of the traditional high thrusting chemical systems. This optimal orbit insertion strategy was found by first using a computer program that finds optimal control schemes for orbit transfers using combined high and low-thrust propulsion systems and calculates the mass and total transfer time of the object at final orbit. This computer program was used to calculate final mass and time values for an orbit transfer from LEO to GEO using various orbit insertion strategies that required incremental amounts of SEP Δv. Next, a model was created which used the data from the computer program to calculate final *available* spacecraft mass and total orbit insertion cost. Final available spacecraft mass, total transfer time, and total orbit insertion cost were the only three mission attributes considered in finding optimal solutions for this effort. Utility functions which quantify how the values of each mission attribute relate to mission objectives were then created, along with weighting schemes that represent the relative importance of each attribute to the mission. Finally, utility curves were created for numerous examples. From these utility curves the optimal orbit insertion strategies were found. Depending on the utility functions and weightings used in each example, it was determined that SEP systems providing a portion of the orbit transfer was the optimal scenario for many cases.

The computer model used for this effort, SEPSPOT, was more than adequate for determining optimal combined high and low thrust trajectories. Versions of SEPSPOT

that are different than the one used for this effort are reportedly available, with some having improved convergence algorithms and a more user-friendly radiation degradation model for different solar cell types. Regardless of the computer code used, however, it is crucial that one be selected which optimizes *both* a high and low thrust portion of an orbit transfer and accounts for the various perturbations and environmental effects along the way. The computer code should also allow the portion of either the high or low thrust transfer to be assigned by the user and easily varied.

Although the optimal solutions for combined high and low thrust orbit transfers were found using examples for a variety of generic orbit insertion missions, some general trends for optimal solutions were discovered which should not vary, even if the performance parameters and attribute models are changed to more accurately represent an actual space mission. The optimal orbit insertion strategy for any mission which is considering the use of both high and low thrusting propulsion systems is ultimately determined by the desirability of the values for each mission attribute (attribute utility) and the relative importance of each attribute to the mission (attribute weightings). Obviously if transfer time (or final mass available) is of the utmost importance to a mission, then the optimal orbit insertion strategy will simply be to minimize time (or maximize final mass) and only a high thrusting (or low thrusting) propulsion system will be employed. These situations were confirmed by examples in this effort that reflected such mission preferences. Trends that were more interesting to examine occurred when example missions used attribute utility functions and weighting schemes that resulted in optimal orbit insertion strategies requiring the combined use of high and low thrust propulsion

systems. These optimal orbit insertion strategies typically appeared when none of the mission attributes were weighted in Eq (8) so as to dominate the others. Missions which used attribute weightings that were evenly distributed consistently resulted in optimal insertion strategies requiring a combined use of high and low thrust propulsion systems. When the attribute weighting schemes were not evenly distributed, the attribute utility functions played a significant role in determining the types of weighting schemes which resulted in combined high and low thrust orbit transfers. If multiple utility functions rendered consistently high utility scores for a broad range of attribute values, it resulted in the largest range of attribute weighting schemes which had optimal orbit insertion strategies involving both high and low thrust propulsion systems. These types of utility functions are typically exponential and have the shape of Eq (5) and Eq (7). They will render consistently high utility scores for a broad range of attribute values when a large portion of the attribute's range of values is highly desirable. This situation arises because the attribute utility functions will have an area along their curves where they render high utility scores as a function of the same SEP Δv values, thus leading to a high total utility score for that region regardless (to some extent) of the attribute weighting scheme employed.

While SEPSPOT calculated all total transfer times used in this effort, Eq (8) and Eq (9) were used to model the final available mass and total orbit insertion cost attributes respectively. As described in chapter five and six, the spacecraft's final available mass was a value used to reflect the mass penalties associated with various propulsion systems configurations, and the orbit insertion cost accounted for the cost of placing the spacecraft

82

from the launch pad to its final orbit at GEO. While it was the intent of this work to model all mission attributes with reasonably accurate figures, it was not the purpose of this effort to forecast actual optimal orbit insertion strategies for existing or near-term space missions. All models used to compute mission attributes (and the assumed performance specifications) were intended as simple examples only. Establishing methods for finding the optimal orbit insertion strategy using both high and low thrust propulsion systems was the goal of this work and was successfully demonstrated for a variety of mission profiles. Using the methods presented in this work, it is hoped that space mission planners can use their own attribute models, tailored for a specific mission profile, and find the best method of inserting a spacecraft into final orbit when both high and low thrust propulsion systems are available.

Bibliography

1. Clemen, R. T. <u>Making Hard Decisions, an Introduction to Decision Analysis</u> (Second Edition). Belmont CA: Duxbury Press, 1996.

2. Curran, F. M. and L. Callahan. "The NASA On-Board Propulsion Program," AIAA-95-2379, July 1995.

3. Dickey, M. R. and others. "The Electric Vehicle Analyzer (EVA): An Electric Orbit Transfer Vehicle Mission Planning Tool," AIAA-90-2984, August 1990.

4. Edelbaum, T. N. The Use of High- and Low-Thrust Propulsion in Combination for Space Missions," <u>Journal of Astronautical Sciences, 9</u>: 49-60, (1962).

5. Elkins, T. and T. Galati. "ROTV Concepts Analysis," AIAA-96-3016, July 1996.

6. Garrison, James L. "Solar Electric Propulsion for the Orbital Transfer of Large Spacecraft to Geosynchronous Orbit," AIAA-92-4579, August 1992.

7. Gulczinski III, F. S. and R. A. Spores. "Analysis of Hall-Effect Thrusters and Ion Engines for Orbit Transfer Missions," AIAA-96-2973, July 1996.

8. Haxelrigg, G. A. "Optimal Space Flight with Multiple Propulsion Systems," <u>Journal of Spacecraft and Rockets, 5</u>: 1233-1235 (October 1968).

9. Hersh, Michael. Sales Representative, Pressure Systems Corporation, Los Angeles, CA. Telephone interview. 15 August 1997.

10. Isakowitz, Steven J. <u>International Reference Guide to Space Launch Systems</u>. Washington D. C.: American Institute of Aeronautics and Astronautics, 1991.

11. Janson, S. W. "The On-Orbit Role of Electric Propulsion," AIAA-93-2220, June 1993.

12. Keeney, R. L. and Raiffa, H. <u>Decisions with Multiple Objectives: Preferences and Value Tradeoffs</u>. New York: John Wiley & Sons, Inc. 1976.

13. Loftus, J. P. and C. Teixeira. "Launch Systems," in <u>Space Mission Analysis and Design</u> (Second Edition). Ed. Larson, W. J. and J. R. Wertz. Torrance CA: Microcosm, Inc., 1992.

14. McCann, J. M. <u>Optimal Launch Time for a Discontinuous Low Thrust Orbit Transfer</u>. MS thesis, AFIT/GA/AA/88D-7. School of Engineering, Air Force Institute of Technology (AFIT), Wright-Patterson AFB OH, December 1988 (AD-A202693)

15. Meserole, J. S. "Launch Costs to GEO Using Solar-Powered Orbit Transfer Vehicles," AIAA-93-2219, June 1993.

16. Miller, T. M. and G. B. Seaworth. "An Approach to System Optimization for Solar Electric Orbital Transfer Vehicles," AIAA-93-2222, June 1993.

17. Miller, T. M. and R. S. Pell. "Assessment of the Economic Benefits of Solar Electric Orbital Transfer Vehicles," AIAA-93-2218, June 1993.

18. Oleson, S. R. and others. "Advanced Propulsion for Geostationary Orbit Insertion and North-South Station Keeping," <u>Journal of Spacecraft and Rockets, 34</u>: 22–28 (January-February 1997).

19. Oleson, S. R. and R. M. Myers. "Launch Vehicle and Power Level Impacts on Electric GEO Insertion," AIAA-96-2978, July 1996.

20. Oleson, Steven R. "An Analytical Optimization Method for Electric Propulsion Orbit Transfer Vehicles," American Institute of Physics, A94-32883, January 1993.

21. Pollard, J. E. and others. "Electric Propulsion Flight Experience and Technology Readiness," AIAA-93-2221, June 1993.

22. Porte, F. and others. "Benefits of Electric Propulsion for Orbit Injection of Communication Spacecraft," AIAA-92-1955, March 1992.

23. Sackett, L. L. and others. "Solar Electric Geocentric Transfer with Attitude Constraints: Analysis," NASA CR-134927, August 1975.

24. Sackett, L. L. and T. N Edelbaum. "Optimal High- and Low-Thrust Geocentric Transfer," AIAA-74-801, 1974.

25. Sackheim, R. L. and others. "Space Propulsion Systems," in <u>Space Mission Analysis and Design</u> (Second Edition). Ed. Larson, W. J. and J. R. Wertz. Torrance CA: Microcosm, Inc., 1992.

26. Spitzer, Arnon. "Near Optimal Transfer Orbit Trajectory Using Electric Propulsion," AAS-95-215, February 1995.

27. Stechman, Carl. Propulsion Systems Manager, Kaiser-Marquardt, Van Nuys, CA. Telephone interview. 15 August 1997.

28. Tabucanon, M. T. <u>Multiple Criteria Decision Making in Industry</u>. New York: Elsevier Science Publishers, 1988.

29. "The HS 702 Debut," Hughes Communications, Inc. Excerpt from unpublished article, n. pag. WWWeb, http://www.hcisat.com/new/hs702.html. 18 July 1997.

30. Titus, Nathan A. "Optimal Station Change Maneuver for Geostationary Satellites Using Constant Low Thrust," AIAA-94-3771, August 1994.

31. Vaughan, C. E. and R. J. Cassady. "An Updated Assessment of Electric Propulsion Technology for Near-Earth Space Missions," AIAA-92-3202, July 1992.

32. Wertz, J. R. and others. "Reducing the Cost and Risk of Orbit Transfer," AIAA-87-0172, January 1987.

33. Wiesel, W. E. and S. Alfano. "Optimal Many-Revolution Orbit Transfer," <u>Journal of Guidance, Control, and Dynamics, Vol 8</u>: 155–157 (January-February 1985).

34. Wilson, A. <u>Jane's Space Directory, Tenth Edition 1994-95</u>. Surrey England UK: Sentinel House, 1994.

35. Wong, R. "Cost Modeling," in <u>Space Mission Analysis and Design</u> (Second Edition). Ed. Larson, W. J. and J. R. Wertz. Torrance CA: Microcosm Corporation, 1992.

36. Zeleney, Milan. <u>Multiple Criteria Decision Making</u>. New York: McGraw-Hill Book Company, 1982.

Vita

Captain Darren W. Johnson was born on 17 January 1969 in Hot Springs, Arkansas. He graduated from Rhodes College in 1991 with a Bachelor of Arts degree in Physics. After graduation, Captain Johnson was assigned to Phillips Laboratory at Kirtland AFB, New Mexico.

During his tour at Phillips Laboratory, Captain Johnson initially worked on a program to develop a pellet-bed nuclear powered propulsion engine. In October of 1993, Captain Johnson was assigned to the Space Power Branch where he established and led an in-house program to test and evaluate advanced space photovoltaics that were of interest to the Air Force. In January of 1996, Captain Johnson was selected to attend the Air Force Institute of Technology.

In May of 1996, Captain Johnson entered the Air Force Institute of Technology at Wright-Patterson AFB, Ohio. After completion of the required course work and thesis, he graduated in December of 1997 with a Master of Science Space Operations degree. He was subsequently assigned to the 45th Space Launch Operations Support Squadron at Patrick AFB, Florida.

REPORT DOCUMENTATION PAGE

Form Approved
OMB No. 0704-0188

1. AGENCY USE ONLY (Leave blank)	2. REPORT DATE	3. REPORT TYPE AND DATES COVERED
	December 1997	Master's Thesis

4. TITLE AND SUBTITLE

OPTIMAL ORBIT INSERTION STRATEGIES USING COMBINED HIGH AND LOW THRUST PROPULSION SYSTEMS

5. FUNDING NUMBERS

6. AUTHOR(S)

Darren W. Johnson, Capt, USAF

7. PERFORMING ORGANIZATION NAME(S) AND ADDRESS(ES)

Air Force Institute of Technology, WPAFB OH 45433-6583

8. PERFORMING ORGANIZATION REPORT NUMBER

AFIT/GSO/ENY/97D-02

9. SPONSORING/MONITORING AGENCY NAME(S) AND ADDRESS(ES)

Mr. Terence Galati
PL/RK
Edwards AFB, CA 93524

10. SPONSORING/MONITORING AGENCY REPORT NUMBER

11. SUPPLEMENTARY NOTES

12a. DISTRIBUTION/AVAILABILITY STATEMENT

Approved for public release; distribution unlimited

12b. DISTRIBUTION CODE

A

13. ABSTRACT (Maximum 200 words)

Low thrust electric propulsion systems are becoming sufficiently mature to consider their use as primary propulsion for orbital transfer in place of high thrust chemical systems. Instead of facing an either/or situation, it may be advantageous to use both types. This effort demonstrates a technique for finding orbital transfer strategies that use both high and low thrust propulsion systems and which result in optimal tradeoffs of the performance parameters cost of orbit insertion, total orbit transfer time, and available spacecraft mass at final orbit. These performance parameters are calculated as a function of the fraction of orbit transfer from Low Earth Orbit (LEO) to Geosynchronous Earth Orbit (GEO) provided by electric propulsion. Utility analysis is used to analyze each performance parameter and compute a total utility score for each orbit insertion strategy examined. Results from a variety of example space mission profiles yielded optimal orbit insertion strategies requiring both chemical and electric propulsion to provide a fraction of the LEO to GEO orbit transfer.

14. SUBJECT TERMS

Low Thrust, Electric Propulsion, Orbit Transfer
High Thrust, Utility Analysis

15. NUMBER OF PAGES

98

16. PRICE CODE

17. SECURITY CLASSIFICATION OF REPORT	18. SECURITY CLASSIFICATION OF THIS PAGE	19. SECURITY CLASSIFICATION OF ABSTRACT	20. LIMITATION OF ABSTRACT
Unclassified	Unclassified	Unclassified	UL